Full text open access online (Since 2001)

PRINT: ISSN 0972-3757 ONLINE: ISSN 2456-6330
Int J Hum Genet, 26(1): 1-36 (2026)
DOI: 10.31901/24566330.2026/25.01.925

Translational Potential of Exosomal Phytochemicals (EPCs) in Preclinical Framework: A Next Generation Therapeutics for Multiple Sclerosis

Jehanzaib Islam[1,2], Arif Malik[3,4*], Shahzad Ahmad[5], Javeid Iqbal[6], Marvi Marvi[7], Gul Zaib[3], Ayesha Zahid[3,8], Hassan Mohsin[3], Haleema Saadia[9], Faheem Arif[10], Muhammad Waseem[11], Shazia Iqbal[12], Muhammad Amber Fareed[13] and Qurban Ali[14*]

[1]Department of Biosciences, Grand Asian University, Sialkot, Pakistan
[2]Institute of Molecular Biology and Biotechnology (IMBB), The University of Lahore, Pakistan
[3]School of Pain and Regenerative Medicine (SPRM), The University of Lahore, Pakistan
[4]Faculty of Health Sciences, Equator University of Science and Technology, (EQUSaT), Masaka, Uganda
[5]Faculty of Medicine and Health Sciences, The University of Buckingham, Buckingham, UK
[6]School of Pharmacy, Minhaj University Lahore, Pakistan
[7]Department of Pharmacology, Faculty of Pharmacy, University of Balochistan, Quetta, Pakistan
[8]School of Medical Lab Technology (MLT), Minhaj University Lahore, Pakistan
[9]Islam Medical College (IMC), Sialkot, Pakistan
[10]Faculty of Pharmacy, The University of Lahore, Pakistan
[11]Maternal and Children's Health Research Institute, Shunde Women and Children's Hospital, Guangdong Medical University, Foshan, China
[12]Faculty of Medicine and Health Science, The University of Buckingham, Buckingham UK
[13]Clinical Sciences Department, College of Dentistry, Ajman University, Ajman, United Arab Emirates
[14]Department of Plant Breeding and Genetics, Faculty of Agricultural Sciences, University of the Punjab Lahore, Pakistan
E-mail: [1]<jehanzaibislam112@gmail.com>,[2]<arifuaf@yahoo.com>, [3]<shahzad.ahmad@buckingham.ac.uk>, [4]<gulzaibk30@gmail.com>, [5]<ayeshazahid.uol@gmail.com>, [6]<haxxii69@gmail.com>, [7]<Haleemasaadia31@gmail.com>, [8]<faheeemarif@gmail.com>, [9]<javeidiqbalk30@gmail.com>, [10]<marvibaloch66@yahoo.com>, [11]<mm.waseemjee@gmail.com>, [12]<shazia.iqbal@buckingham.ac.uk>,[13]<m.fareed@ajman.ac.ae>, [14]<saim1692@gmail.com>

KEYWORDS Demyelination. Glial activation. Oxidative injury. Signal transduction. Tissue remodelling

ABSTRACT Multiple sclerosis is a chronic inflammatory and neurodegenerative disease characterised by immune deregulation and oxidative stress. Exosomal phytochemicals have emerged as a promising curative avenue due to their anti-inflammatory and neuroprotective properties. This study examined the therapeutic potential of exosomal phytochemicals in a preclinical rat model of Multiple sclerosis by measuring their effects on inflammatory cytokines, matrix metalloproteinases, heat shock proteins, oxidative stress markers, and molecules active in Multiple sclerosis pathogenesis. A cost-effective in-silico method was developed to predict therapeutic targets, including molecular docking, protein-ligand complexes, phytochemical property analysis, drug likeness, and toxicity prediction. Five out of twenty-two high-potential phytocompounds were selected for further analysis. exosomal phytochemicals treatment significantly reduced pro-inflammatory cytokine levels, oxidative stress markers, and NADPH oxidase activity while enhancing vitamin D3 levels, indicating neuroprotective and immunomodulatory effects. Future studies should focus on molecular mechanisms and clinical validation.

Address for correspondence:
E-mail: arifuaf@yahoo.com; saim1692@gmail.com

INTRODUCTION

Multiple sclerosis (MS) is a chronic, immune-mediated neurodegenerative disease characterised by demyelination, axonal damage, and neuroinflammation within the limits of the central nervous system (CNS) (Haase and Linker 2021). The current curative approach focuses primarily on immunomodulation and symptom management, but so far, they have not been able to change by reversal of neurodegeneration or support remyelination (Iranpanah et al. 2023; Milo et al. 2020). More and more evidence suggests that endothelial progenitor cells (EPCs) retain a significant translational potential for MS therapy by supporting neurovascular repair and modulating immune responses (Tremlett and Marrie 2021). This critique summarises key results from recent investigations on the position of EPCs in Member States, their curative mechanism, and preclinical progress in a rat model. MS pathogenesis is influenced by a complex interaction of biological sensitivity, ecological factors, and a deregulated immune reaction targeting the myelin sheath (Bayat et al. 2021; Javanbakht et al. 2023). Endothelial dysfunction detected in MS patients adds to brain blockade (BBB) upheaval and neuroinflammation (Bhatti et al. 2023; Woodfin et al. 2024). EPCs, a subset of root cells that originate in the bone marrow, have been shown to restore vascular integrity and have immunomodulatory properties (Gresitã et al. 2025).

EPCs may migrate to the site of the CNS injury, separate into endothelial cells, and increase angiogenesis, thus reducing the neurovascular damage. EPCs play a key role in modulating immune responses in MS. They were shown to lower the infiltration of autoreactive T cells and suppress the secretion of proinflammatory cytokines such as TNF- and IL-6 while promoting the release of anti-inflammatory cytokine IL-10 (Beitz et al. 2022; Kaur et al. 2024). Preclinical studies on experimental autoimmune encephalomyelitis (EAE) rat models, a widely used MS model, have shown that EPC therapy alleviates neuroinflammation and improves clinical outcomes (Kaur et al. 2024). EPCs contribute to neurorepair by increasing endothelial cell proliferation, vascular endothelial expansion factor (VEGF), and oligodendrocyte precursor cell differentiation (Mbatha et al. 2023). The EPC-derived exosomes contain bioactive molecules promoting myelin renewal and oxidative stress in demyelinated lesions (Tran et al. 2022).

In vivo studies using a rat model have shown that the EPC transplant leads to improved remyelination and functional recovery. Recent progress in preclinical rat models has made it easier to understand EPC-mediated neuroprotection in MS. Hereditary and pharmacological alterations have been used to increase EPCs' fortitude, migration, and functional efficacy in MS models (Alam 2023; Hatami et al. 2024). These tactics, such as nanoparticle-loaded EPCs and genetically edited EPCs, have shown promise in improving curative results by improving the repair of the BBB and reducing the inflammation of the CNS. However, with promising preclinical results, many challenges remain in the clinical translation of EPC-based therapy in MS. Restricted use of EPCs, moral issues about root cell therapy, and potential rejection of the immune system are among these (La Rosa et al. 2023; Bahrami et al. 2020). To assess safety and efficacy, future studies should prioritise improving EPC transport procedures, cell resilience post transplantation, and supervision of large-scale clinical trials (Malik et al. 2025; Xu et al. 2021). EPCs are a next-generation curative plan for MS, providing both neurovascular repair and immunomodulation. A compelling indication for the efficacy of EPCs in alleviating MS pathology is provided by preclinical rat model surveys. More analysis is needed to accelerate the Polish EPC therapy and accelerate its clinical use in MS patients (Liu et al. 2022; Safir et al. 2025).

Objectives

The study aimed to evaluate the therapeutic potential of exosomal phytochemicals (EPCs) in multiple sclerosis by assessing their effects on inflammation, oxidative stress, and related molecular targets through preclinical and in-silico analyses.

MATERIAL AND METHODS

Study Design and Experimental Site

To assess the curative potential of exosomal phytochemicals in a rat model of multiple sclerosis (MS), an experimental investigation was conducted at the School of Pain and Regenerative Medicine (SPRM), The University of Lahore.

Animal Model and Ethical Approval

The study included 80 female Sprague Dawley rats aged 6-8 weeks. Ethical approval was obtained from The University of Lahore's Institutional Review Board. The rats were maintained under standard housing conditions with ad libitum access to food and water.

MS Induction

MS was induced in the rats using an established experimental autoimmune encephalomyelitis (EAE) protocol. The induction was confirmed through clinical scoring and histopathological analysis.

In Silico Studies

The toxicity and pharmacokinetics of exosomal phytochemicals were evaluated through in silico computational approaches. ADMET (absorption, distribution, metabolism, excretion, and toxicity) predictions were performed using molecular docking, pharmacokinetics modelling, AdmetSAR, SwissADME, IMODE and predictive algorithms to assess bioavailability and potential off-target effects.

Data Retrieval

The uniport (https://www.uniprot.org/) and PDB (https://www.rcsb.org/) databases were utilised to retrieve 44 recipient protein structure in PDB format and the tool discovery studio visualiser employs to purify the protein like the removal of heat, water molecule, ligand group and other impurities, and then add the polar hydrogen to the protein. The NCBI tool PubChem (https://pubchem.ncbi.nlm.nih.gov/) was used to download the SDF format of the phytocompounds (Ligands) for further analysis.

Molecular Docking Analysis

For docking analysis, PyRx (https://sourceforge. net/projects/pyrx/) was used. For docking load, the protein was converted into macromolecules. The vine window was used to upload the ligands one by one, check and note the dimensions X, Y, Z and add a grid box that covered the specified area of processed protein for docking then run the vine wizard (Roy et al. 2024; Safir et al. 2025).

Protein Ligand Complexes

The Macromolecule file retrieved from the docking result load the docked file of the protein and compound was opened using the Discovery studio visualiser (https://www.3ds.com/products/biovia/discovery-studio) (Petersen et al. 2021; Banerjee et al. 2024) and make a complex between protein and ligand using interaction window, convert in to 2D view, note the interactive points occurring in amino acid levels and note the bindings for hydrophobic, hydrophilic, hydrogen, covalent hydrogen, alkyl, pi-alkyl, sigma, pi-sigma, wander walls, etc. and save the protein ligand complex in PDB format for further analysis.

Phytochemical Analysis

The AdmetSAR (https://lmmd.ecust.edu.cn/admetsar1/about/) server was employed to identify the phytochemical properties of the compounds. Selected compounds have high phytochemical properties, the ability to cross Blood Brain Barrier (BBB) and potential Human Intestinal Absorption (HIA+). To validate whether the phytocompounds are able to cross the (BBB+) and the drugable property, SwissADME was used. SwissADME (http://www.swissadme.ch/) apprises the drug likeness properties of the short-listed compounds. Target compounds obey the Lipinski Rule of Five (Rule of Law) and also validate the potential property to cross +BBB (Alimohammadi et al. 2022).

Toxicity Prediction

Compounds were shortlisted on the basis of molecular docking, AdmetSAR, and SwissADME, that are non-toxic, non-carcinogenic, non-hepato, muta, and cytotoxic to the human body. For toxicity analysis, ProTox-3 (https://tox.charite.de/protox3/index.php?site=compound_input) was utilised. Shortlisted phytocompounds (drug) have specified therapeutic properties (Okon 2024).

Dynamic Simulation

Protein and various other molecules are always moving and not static in nature. A dynamic

analysis of the protein was conducted to validate the deformability, beta factory, eigenvalues, elasticity, covariance map and variance analysis of the PDB file retrieved from the complex analysis of the recipient protein and the phytocompounds (Ginwala et al. 2019; Yildirim et al. 2023), using the Discovery studio visualiser and for the dynamic analysis, IMODE database (https://imods.iqf.csic. es/) was used. This study was followed by Gaur and Siddique (2024).

Treatment Groups and Interventions

After MS confirmation, the rats were randomly divided into eight groups (n=10 per group) and treated for four weeks via intraperitoneal (IP) injection. Diroximel fumarate served as the standard drug control.

Table 1: Experimental design

Groups	*Treatment*	*Dose and route*
G1	Control (Untreated)	No treatment
G2	Exosome Vehicle Only	100 µL IP
G3	Onosmin-Exosome	50 mg/kg IP
G4	THC-Exosome	05 mg/kg IP
G5	Naringenin-Exosome	50 mg/kg IP
G6	Apigenin-Exosome	50 mg/kg IP
G7	Stigmasterol-Exosome	50 mg/kg IP
G8	Diroximel Fumarate	05 mg/kg IP

Exosome Isolation and Phytochemical Loading

Human mesenchymal stem cells were cultured in Dulbecco's modified Eagle medium (DMEM) supplemented with 10 percent exosome-depleted foetal bovine serum (FBS) and 1 percent penicillin-streptomycin. Cells were kept at 37°C in a humidified incubator with 5 percent CO2 and transferred to reach 80 to 90 percent confluence. The society medium was replaced every 48 days, and the conditioned medium was prepared after 72 days of incubation.

Exosome Isolation by Ultracentrifugation

The collected conditioned medium was subjected to a multi-step differential centrifugation process to isolate exosomes as follows. To remove cell debris, a low-speed centrifuge was performed with 300 grams of medium for 10 minutes at 4°C. To extinguish the apoptotic body and larger extracellular vesicle, the supernatant was centrifuged at a rate of 2,000 grams for 20 minutes at 4°C. High-speed centrifugation of the clarified supernatant was performed in an ultracentrifuge with an Optima XPN-100 ultracentrifuge (Beckman Coulter, USA) with a type 70 Ti rotor for 70 minutes at 4°C. The pellet was resuspended in a phosphate-buffered saline solution (PBS) and ultracentrifuge once more at close to 100,000 grams for 70 minutes at around 4°C to remove the contaminants. The purified exosome pellet was resuspended in 100 L PBS and stored at -80°C for further word pictures and experiments.

Exosome Characterisation

Transmission Electron Microscopy (TEM)

Morphological study of exosomes using TEM. The release of exosome suspension was placed on a carbon-coated copper grid and followed for 10 minutes, then negative staining with 2 percent uranyl acetate for contrast enhancement was conducted. The grid has been dried and analysed under the JEOL JEM-2100 electron microscope at a voltage of 80 kV.

Dynamic Light Scattering (DLS)

The Zetasizer Nano ZS from Malvern Instruments, UK was used to study the hydrodynamic diameter and size distribution of isolated exosomes. Exosomes were diluted in PBS, and measurements were made at 25 C with a dispersal angle of 173°.

Nanoparticle Tracking Analysis (NTA)

The NS300 NTA organisation NanoSight and Malvern Instruments, United Kingdom was used to measure exosome concentration and size distribution. The exosome suspension was diluted to 1:100 in PBS, injected into the sample chamber, and measured under the laser beam. The average size and concentration of atoms were analysed using NanoSight software.

Phytochemical Loading Into Exosomes

Selection of Phytochemicals

The phytochemicals selected to load into exosomes were listed by the specific phytochemi-

cals, for example, curcumin, resveratrol, and quercetin based on their known curative properties and bioavailability.

Sonication-Assisted Loading Method

Exosome loading with phytochemicals was performed using a sonication method to enhance bioavailability and stability. The preparation of the phytochemical solution The phytochemicals were dissolved in dimethyl sulfoxide (DMSO), otherwise a suitable solvent, and diluted to achieve a final concentration of 10 M in PBS. In a 1:1 ratio, isolate exosomes were incubated with a phytochemical solution. The mixture was subjected to three stages of sonication (20 kilohertz for 30 seconds respectively, using a probe sonicator Qsonica Q700, USA) and a two-minute cooling interval between circles to prevent overheating. The sonicated exosome-phytochemical in question was incubated for 1 hour at 4°C to facilitate encapsulation, followed by ultracentrifugation at 100,000 grams for 70 minutes near 4°C to remove unincorporated phytochemicals. The final pellet was resuspended in PBS and stored at -80 C for further examination.

Verification of Phytochemical Loading

High-Performance Liquid Chromatography (HPLC)

To verify phytochemical encapsulation in exosomes, HPLC was performed. Firstly, exosomes were lysed in a buffer containing a detergent, and the phytochemicals obtained were analysed using an Agilent 1260 Infinity HPLC system equipped with a C18 column. The transportable phase of acetonitrile and water was adjusted to a pH of 3.0 with 0.1 percent formic acid, and the detection was carried outside near the nanometer wavelength. The researchers compared retention times and peak zones with standard phytochemicals.

Fluorescence Microscopy

To visualise load performance, phytochemically loaded exosomes were labelled with a fluorescent dye (DiO, DiI) and detect less than a fluorescence microscope (Leica DMi8, Germany). The exosomes were incubated for 30 minutes at room temperature, washed with PBS and imaged below the appropriate excitation and emission wavelengths.

Biomarker Analysis

Serum and tissue samples were collected for the analysis of various biomarkers associated with MS pathophysiology, neuroinflammation, and oxidative stress. The quantified biomarkers included TNF-α, MMP-9, HSP27, Integrin α4β1, MMP-2, VCAM-1, TGFα1, HSP32, SOD, CAT, HSP90, HSP60, MMP-3, MOG, Vitamin D3, 4-HNE, sNfL, MBP, DHODH, PAD4, LCN2, Beclin-1, 8-OHdG, PLP1, PAD2, Lingo-1, HSP70, Protein Carbonyls, MDA, IsoP-F2α, IL17AF, Nogo-A, GFAP, HSPB5, Amyloid-β (Aβ), NADPH Oxidase, GSH, CXCL10, LC3-II, IL6, and IL1βusing Elisa kits.

Histopathological Studies

Tissue Collection and Fixation

Tissue samples (from the brain) were collected from the experimental and restraint cohort under sterile conditions and immediately repaired with 10 percent neutral-buffered formalin for 24-48 hours in order to maintain the cellular architecture. After arresting development, the tissues were washed in phosphate-buffered saline solution (PBS) to remove excess fixative and to dehydrate in a graded ethyl alcohol series of 70 percent, 80 percent, 90 percent, 95 percent, and 100 percent.

Tissue Processing and Embedding

The dehydrated tissues were uncluttered with xylene and then implanted in paraffin wax to facilitate sectioning. The paraffin block was then cooled and segmented into 4-5 m middle slices using a rotatable microtome.

Staining Procedures

The tissue sections were placed on a glass slide, deparaffinised in xylene, and rehydrated by a descending ethanol series. In order to assess general tissue architecture and morphologic variations, a histopathological assessment was performed using hematoxylin and Eosin staining. Other staining methods, such as Masson's Trichrome

staining of collagen formation and Periodic Acid-Schiff staining of glycogen and mucopolysaccharide, were used if necessary.

Microscopic Examination

Cellular morphology, tissue virtue, inflammatory infiltration, fibrosis, and alternative pathological changes were assessed by analysing the stained tissue sections inferior to a light microscope, Olympus/Leica, at a magnification of several microns to measure cellular morphology, tissue virtue, inflammatory infiltration, fibrosis, and alternative pathological changes. A high-resolution virtual camera attached to a microscope was used to take representative photographs.

Quantitative Histopathological Analysis

ImageJ was used to measure parameters such as inflammatory cell infiltration, fibrosis index, and tissue damage. The blind diagnostician shall measure the histological score using a standardised scale.

Statistical Analysis

All statistical analyses were performed using SPSS software (version XX, IBM, USA) and GraphPad Prism (version XX, GraphPad Software, USA). Data were expressed as mean ± standard deviation (SD). The normality of the data was assessed using the Shapiro-Wilk test. One-way analysis of variance (ANOVA) was applied to compare the means across different experimental groups, followed by post-hoc least significant difference (LSD) tests to determine pairwise differences. A significance level of $p \leq 0.05$ was considered statistically significant.

RESULTS AND DISCUSSION

In-Silico Results

The purified protein and ligand retrieved from the tools were processed for docking analysis (La Rosa et al. 2023). MD shows that the total of 5 (Onosmin, THC, Naringnin, Apigenin, and Stigmasterol) phytocompounds out of 22 were screened (Supplementary Table 1 and Table 5) as a potential

Table 2: Docking result of shortlisted compounds

	Phytocompounds				
Protein	*Onosmin*	*THC*	*Naringnin*	*Apiginin*	*Stigmasterol*
MMP-3			-9.3	-9.2	
DHODH	-9.5	-9.4	-9.8	-9.8	
MMP-2					-9.6
MMP-9			-9.6	-9.7	

Table 3: Binding affinity and binding interaction of phytocompounds with recipient proteins

Protein	*Phytocompounds*	*Binding Affinity*	*Bond*	*Category*
MMP-3	Naringnin	-9.3	Covalent Hydrogen	Conventional hydrogen bond, Pi-Pi T-shaped, Pi-Pi Stacked
	Apiginin	-9.2	Hydrogen	Van der Waals, Pi-Pi T-shaped, Pi-Alkyl
DHODH	Onosmin	-9.5	Covalent Hydrogen	Van der Waals, Covalent bond, conventional hydrogen bond
	THC	-9.4	Covalent Hydrogen	Van der Waals, conventional hydrogen bond, Pi-Alkyl, Amide-Pi Stacked
	Naringnin	-9.8	Hydrogen	Van der Waals, Pi-Alkyl
	Apiginin	-9.8	Covalent Hydrogen	Van der Waals, conventional hydrogen bond, Pi-Alkyl, Amide-Pi Stacked, Carbon Hydrogen Bond
MMP-2	Stigmasterol	-9.6	Hydrogen	Van der Waals, Pi-Alkyl
MMP-9	Naringnin	-9.6	Covalent Hydrogen	Van der Waals, conventional hydrogen bond Pi-Alkyl
	Apiginin	-9.7	Covalent Hydrogen	Van der Waals, conventional hydrogen bond, Pi-Alkyl, Pi-cation

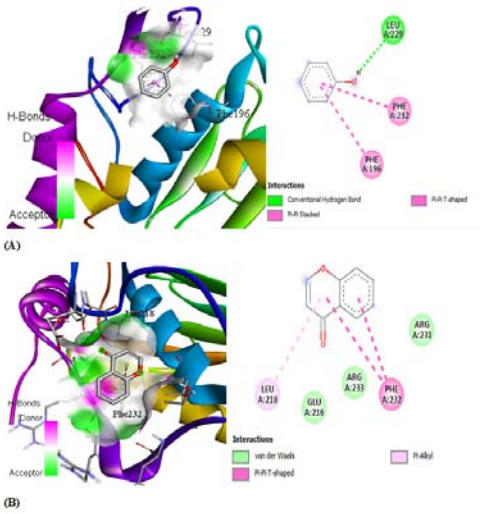

Fig. 1. MMP-3 complex with Naringin and Apiginin

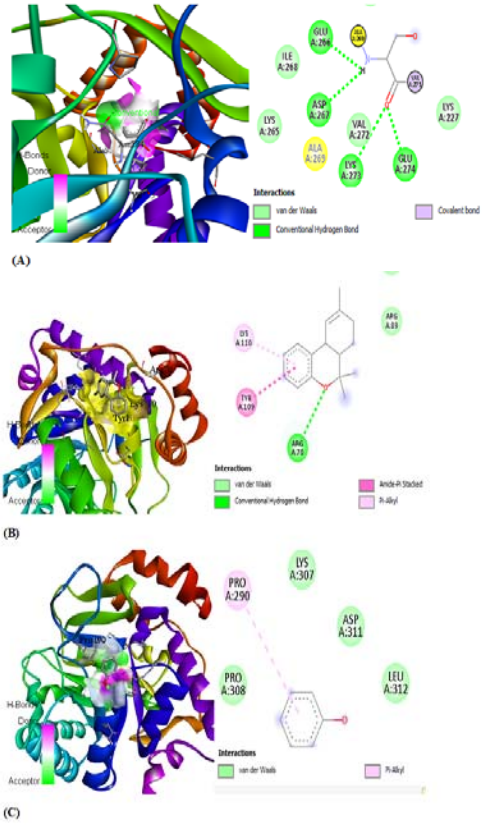

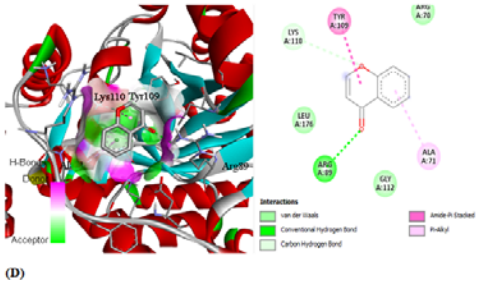

Fig. 2. DHODH complex with Onosmin, THC, Naringnin, Apiginin

drug candidate against the recipient protein MMP-3 (-9.3, -9.2) having dimensions X:46.68, Y:43.74, Z:46.03, DHODH (-9.5, -9.4, -9.8, -9.8) having dimensions X:58.09, Y:63.39, Z:64.42, MMP-2 (-9.6) dimensions X:82.97, Y:69.00, Z:86.63, MMP-9 (-9.6,-9.7) having dimensions of X:47.68, Y:48.11, Z:49.52. Selected ligands have a high binding affinity and low binding energy as shown in Table 2. Table 3 shows further analysis in Discovery studio for recipient protein and the phytocompounds on the basis of amino acid residue level. As shown in Figure 1 to 4, MMP-3 interact with naringnin and apigenin on residue (LEU:229, PHE:232, PHE:196, PHE:332, LEU:218), DHODH bind with onosmin, THC, Naringnin, Apiginin, and Stigmasterol on A.A residue (ALA:269, VAL:271, GLO:266, ASP:267, LYS:273, GLU:274, LYS:110, TYR:109, ARG:70, PRO:290, LYS:110, ALA:71, ARG:89), MMP-2 interaction analysis with stigmasterol having residue (PHE:331, TYR:314), and MMP-9 binding complex with Naringnin and Apiginin in the residue (ARG:424, LEU:397).

Phytochemical Analysis

The total 22 phytocompounds were docked and 13 ligands were obtained with probable value for further analysis. Phytochemical characteristic analysis of compounds was determined by using AdmetSAR. 5 (Onosmin, THC, Naringnin, Apiginin, Stigmasterol) compounds out of 13 were selected as a potential drug candidate. Shortlisted phytocompounds on the basis of properties like, Bain-Blood Barriers+, Intestinal Absorption (HIA+), Caco+2 Permeability, P-glycoprotein, P-glycoprotein Inhibitor, Biodegradation, Aqueous solubility

(Logs) and AMES Toxicity as shown in Supplementary Table 2 and Table 3. To validate the prediction further, the tool Swiss ADME was used to check the pharmacokinetic properties of the drug candidates on the basis of Lipinski rule of five molecular weight (d"500), H-bond acceptors (≤10), H-bond doners(≤5), MR(≤40-130), Silicos-IT Log P (≤5), Atoms, Lipinski #violations, and BBB+ as shown in Supplementary Table 3i-ii. The selected phytocompounds have potential properties to cross the blood brain barrier and suppress or inhibit MS according to in-silico studies.

Toxicity Prediction

Toxicity prediction is an important in drug development, as ProTox-3 utilisation of the potential drug predicts various endpoints like chemical safety, skin irritations, carcinogenicity, environmental health, immunogenicity, mutagenicity, were all these steps prioritise safer compounds for in-vivo studies. Selected phytocompounds are safe and non-toxic to the human body, and were able to use in-vivo studies shown in Supplementary Table 4.

Dynamic Studies

For protein-ligand dynamics analysis IMODE were utilised. Figure 5 shows the simulation analysis of high potential phytocompounds, Naringnin and Apiginin, and the dynamic property of the complex. The flexibility of a molecule at all of its A.A residue of the shortlisted phytocompounds is described by its main-chain deformability. High deformability regions of the protein-ligand frequently serve as "hinges", facilitating easier bending or movement of the molecule to inhibit and deform the target. The PDB (phytocompounds complex) file is typically used to extract the experimental B-factor, which represents atomic mobility. The B-factor for structure analysis to Normal Mode Analysis (NMA) is obtained by multiplying the NMA mobility by (8pi^2). It is important to keep in mind that averaged root-mean-square (RMS) values are frequently seen in the B-factor column of complex files from NMR experiments rather than actual B-factors. Eigenvalues indicate the stiffness of a structure's motion, with lower eigenvalues suggesting easier deformations and larger eigenvalues suggesting stiffer, more rigid motions. Eigenvalues have an inverse relationship with variance, with higher variances observed in modes with lower eigenvalues. Individual variances are represented by red bars, while cumulative variances are shown by green bars, allowing for better understanding of a structure's total flexibility. The covariance matrix shows the movement of residue pairs, indicating anti-correlated, uncorrelated, or correlated movements. It is computed using Cα atomic coordinates. The elastic network model (Hatami et al. 2024) depicts atomic interactions as springs, with each dot representing a spring joining two atoms. The colour of the dot indicates the rigidity of the spring, making it easier to understand the

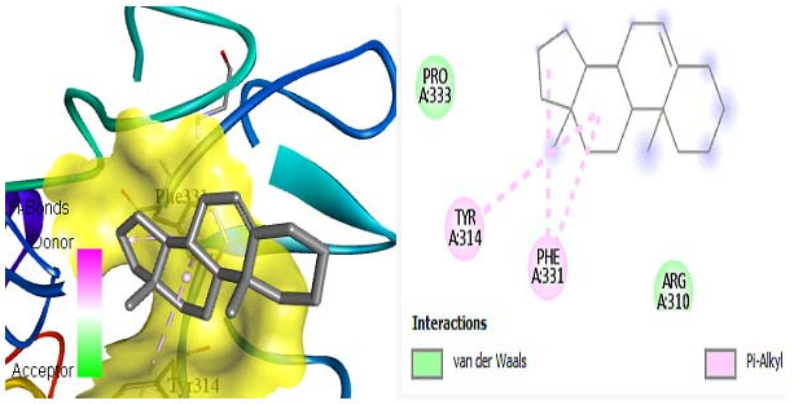

Fig. 3. MMP-2 interacts with Stigmasterol

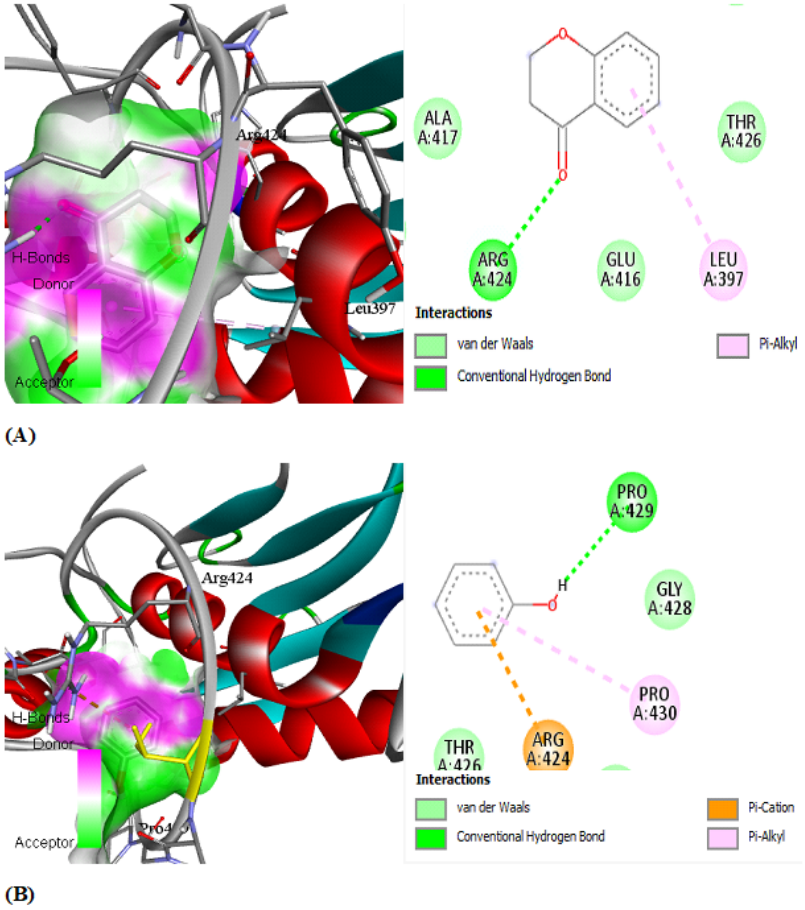

Fig. 4. MMP-9 Complex with Naringnin and Apiginin

Table 4: Comparative analysis of histopathological studies under exosomes loaded phytochemicals

Group	*Remyelination (LFB Staining)*	*Oligodendrocyte Density (PAS Stain)*	*Neuroinflammation reduction*	*Axonal integrity*
G1 (Untreated EAE)	Severe myelin loss	Severe depletion	High perivascular inflammation	Severe damage
G2 (Exosome Vehicle)	Minimal improvement	Low density	Mild reduction	Moderate damage
G3 (Onosmin-Exosome)	Moderate preservation	Moderate density	Reduced inflammation	Improved
G4 (THC-Exosome)	Mild to Moderate	Moderate	Strong anti-inflammatory effect	Good
G5 (Naringenin-Exosome)	Marked remyelination	High oligodendrocyte density	Minimal inflammation	Excellent
G6 (Apigenin-Exosome)	High remyelination	Very high density	Strong Anti-inflammatory	Excellent
G7 (Stigmasterol-Exosome)	Moderate remyelination	Moderate density	Mild inflammation reduction	Good
G8 (Diroximel Fumarate)	Moderate remyelination	Moderate to high	Significant inflammation reduction	Good

physical interactions that maintain a molecule's structural stability (Supplementary Figure 1-4).

Biochemical Studies

The inflammatory and molecular modulation in multiple sclerosis (MS)-induced rats was significantly altered following treatment with exosomal phytochemicals (EPCs), as demonstrated across multiple immunomodulatory and stress-responsive biomarkers (Figure 6, and Supplementary Table 6). Tumour Necrosis Factor-alpha (TNF-α) levels were significantly elevated in the MS-induced exosome vehicle group (45.88±8.49 pg/mL) compared to the healthy control (21.25±5.66 pg/mL). Among the EPC-treated groups, Naringenin-Exosome (24.59±4.49 pg/mL) and THC-Exosome (27.59±5.19 pg/mL) demonstrated a significant reduction in TNF-α (p=0.021). Similarly, Interleukin-6 (IL-6) levels were markedly increased in the diseased group (35.21±6.29 pg/mL), while Naringenin- and THC-loaded exosomal treatments effectively restored IL-6 levels to near-normal (15.79±3.55 pg/mL and 18.89±3.78 pg/mL, respectively) (p=0.032). IL-17AF and IL-17 were notably elevated in the positive control group (22.49±3.95 pg/mL and 20.33±3.72 pg/mL, respectively), while all EPC formulations significantly attenuated their expression. Naringenin-Exosome treatment reduced IL-17AF and IL-17 to 9.99±2.21 pg/mL and 9.55±1.89 pg/mL, respectively (p=0.028, p=0.025).

IL-1β followed a similar trend, being suppressed by Naringenin and THC-based EPCs from 31.55±4.89 pg/mL in the diseased group to 14.88±2.55 pg/mL and 16.59±2.98 pg/mL, respectively (Fig. 6, p=0.030). Heat Shock Proteins (HSPs) were prominently upregulated in the MS group, with HSP27, HSP60, HSP70, and HSP90 showing significant increases. In contrast, Naringenin-Exosome treatment led to a marked reduction in HSP27 (20.15±3.79 pg/mL), HSP60 (14.92±2.99 ng/mL), HSP70 (12.35±2.55 ng/mL), and HSP90 (18.75±3.42 ng/mL), with statistical significance across all comparisons (p=0.027, 0.031, 0.028, and 0.026, respectively). Regarding matrix metalloproteinases (MMPs), MMP-9, MMP-2, and MMP-3 were all elevated in the disease control group (35.42±5.78, 27.88±4.99, and 19.65±3.55 ng/mL, respectively). EPC interventions, particularly Naringenin-Exosome (16.75±2.98,

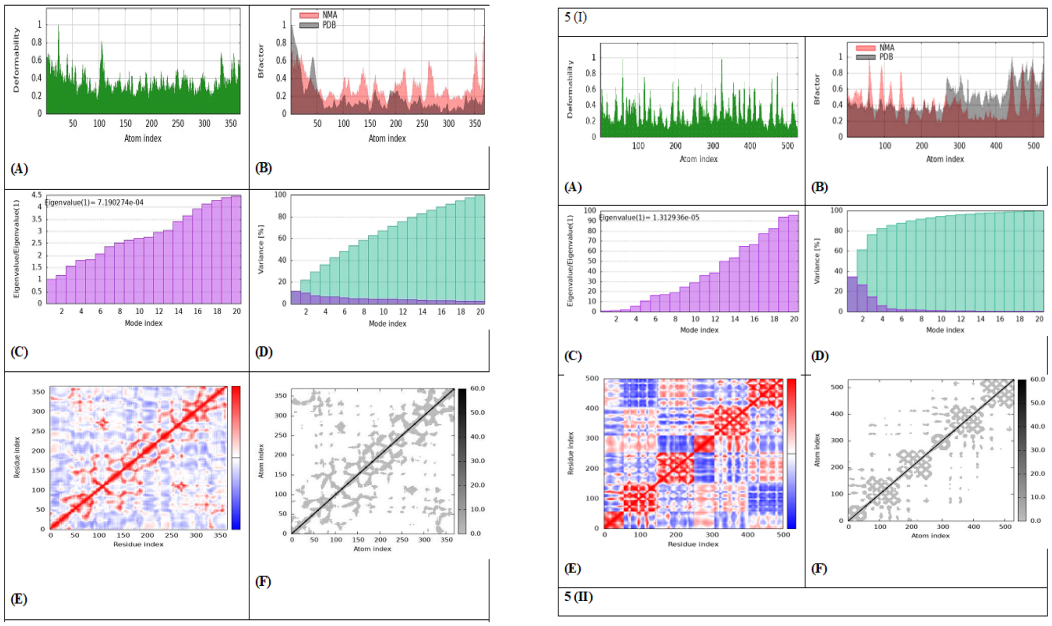

Fig. 5 I-II. Dynamic analysis of the protein DHODH Complex with Naringnin and Apiginin

13.42±2.65, and 8.99±2.11 ng/mL), effectively downregulated these proteolytic markers (Fig. 6; p=0.027, 0.034, and 0.029, respectively), suggesting preservation of blood brain barrier integrity and reduced neuroinflammation. A significant upregulation ($p \leq 0.018$) of Integrin $\alpha 4\beta 1$ was observed in the MS-induced+Control group (22.88±3.99 ng/mL), which was markedly downregulated in Naringenin-Exosome (11.55±2.35 ng/mL) and THC-Exosome (12.99±2.55 ng/mL) treated groups (Fig. 7a-h, and Supplementary Table 7). Likewise, VCAM-1 expression was significantly elevated in the +Control group (34.42±5.78 ng/mL), while Naringenin (18.75±3.55 ng/mL) and Apigenin-Exosome (23.35±4.22 ng/mL) interventions demonstrated substantial suppression ($p \leq 0.025$, Fig. 7b).

TGFβ1 levels also rose significantly in the MS+Control group (40.25±5.99 pg/mL), whereas Onosmin-Exosome (30.99±4.35 pg/mL) and Apigenin-Exosome (28.55±4.78 pg/mL) showed meaningful reduction ($p \leq 0.021$, Fig. 7c). In terms of oxidative stress, NADPH Oxidase activity reached 19.65±3.55 µmol/min/mg in the +Control group and was notably reduced in Naringenin (8.99±2.11 µmol/min/mg) and THC-Exosome (10.25±2.55 µmol/min/mg) treatments ($p \leq 0.019$, Fig. 7d). Supplementation with EPCs positively modulated Vitamin D3 levels, with significant elevation seen in Naringenin (24.75±3.99 ng/mL) and THC-Exosome (22.99±3.78 ng/mL) compared to the MS+Control (12.42±3.35 ng/mL; $p \leq 0.022$, Fig. 7e). Similarly, HSP32 was markedly decreased by EPCs, with Naringenin-Exosome (16.89±3.25 ng/mL) and THC-Exosome (19.35±3.42 ng/mL) groups showing reduced levels versus the MS+Control (30.55±5.19 ng/mL; $p \leq 0.024$, Fig. 7f). Protein Carbonyls, a marker of protein oxidation, surged in the +Control group (4.88±1.02 nmol/mg), yet were significantly reduced following treatment with Naringenin-Exosome (2.42±0.65 nmol/mg; p=0.019, Fig. 7g). NF-êB, a critical transcription factor in MS pathophysiology, was upregulated in MS rats (38.42±5.78 pg/mL) but significantly inhibited by Naringenin (21.75±3.42 pg/mL) and Apigenin-Exosome (26.35±4.11 pg/mL) treatments ($p \leq 0.022$, Fig. 7h).

Lipid peroxidation marker MDA was significantly elevated in MS-induced rats (7.99±2.35 nmol/mL), while EPCs, especially Naringenin (4.25±1.11 nmol/mL) and THC-Exosome (4.99±1.32 nmol/mL), effectively suppressed it (pd"0.020, Fig. 7i). Similarly, 8-OHdG, a DNA oxidative damage marker, decreased significantly with Naringenin (5.42±1.55 ng/mL) and THC-Exosome (6.15±1.75 ng/mL) treatments compared to the +Control (10.25±2.88 ng/mL; $p \leq 0.021$, Fig. 7j). EPCs also reduced IsoP-F2α levels ($p \leq 0.023$), with Naringenin-Exosome-treated rats (15.75±3.11 pg/mL) showing a prominent drop relative to the +Control (29.55±4.89 pg/mL; Fig. 7k). Notably, SOD activity, which was suppressed in MS-induced rats (7.88±2.45 U/mg), was significantly restored in Naringenin (16.35±3.78 U/mg), THC-Exosome (14.22±3.45 U/mg), and Stigmasterol-Exosome (14.88±3.55 U/mg) treated groups ($p \leq 0.018$, Fig. 7l). A significant decrease (p=0.020) in catalase (CAT) levels was observed in the MS+Control group (10.55±3.12 U/mg) compared to the healthy Control group (25.75±4.55 U/mg), indicating elevated oxidative stress (Fig. 8a-l, and Supplementary Table 8). However, treatment with Naringenin-Exosome notably restored CAT levels to 23.75±4.78 U/mg, reflecting potent antioxidant properties. Myelin oligodendrocyte glycoprotein (MOG) levels were significantly elevated (p=0.021) in the MS+Control group (15.22±2.88 ng/mL), suggesting active demyelination (Fig. 8b).

Among all EPCs, Naringenin- and THC-Exosomes exhibited pronounced reduction in MOG expression (7.55±1.99 and 8.99±2.11 ng/mL, respectively), demonstrating their remyelinating potential. The lipid peroxidation marker 4-HNE showed a marked increase in the MS+Control group (8.75±2.42 nmol/mL), significantly reduced by EPCs administration (p=0.022). Naringenin- and THC-Exosome groups displayed lower 4-HNE levels (4.25±1.32 and 4.99±1.55 nmol/mL, respectively), closely aligning with the normal range (Fig. 8c). Serum neurofilament light chain (sNfL), a neuronal injury marker, was significantly upregulated (25.35±4.88 pg/mL) in MS-induced rats (p=0.023). EPCs especially Naringenin (13.42±3.22 pg/mL) and THC (15.88±3.42 pg/mL) significantly attenuated sNfL levels (Fig. 8d). Regarding Myelin Basic Protein (MBP), significant degradation was observed (Supplementary Table 9) in the MS+Control group (19.24±2.98 ng/mL), compared to 42.59±3.12 ng/mL in healthy controls (p=0.018). Naringenin and THC treatments preserved MBP levels at 40.24±3.76 and 38.79±4.02

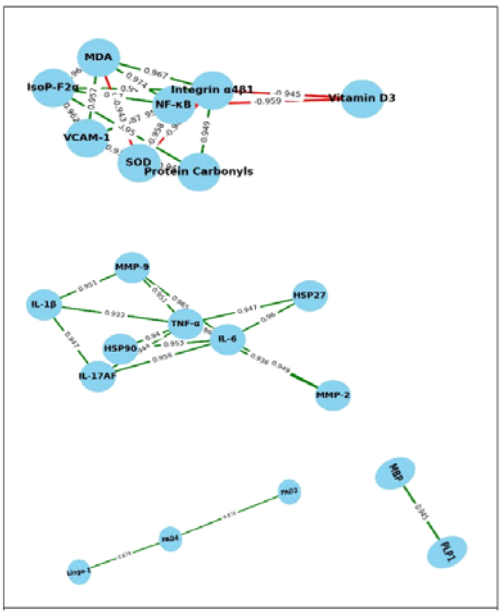

Fig. 6. Network graph illustrating highly correlated variables (|r| > 0.95)
Nodes represent biomarkers
Edges show strong correlations with **green lines:** Positive correlations and **red lines:** Negative correlations.
Edge labels: Pearson correlation values

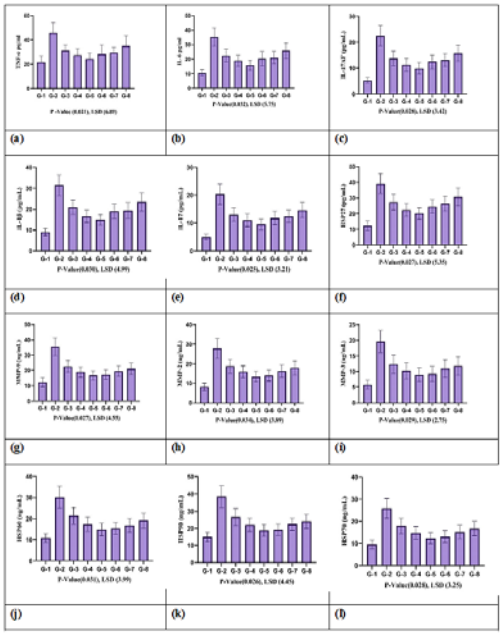

Fig. 7. Levels of TNF-á, IL-6, IL-17A, IL-1â, IL-17, HSP27, MMP9, MMP2, MMP3, HSP60, HSP90 and HSP70 in MS-induced rats treated with Exosomal Phytochemicals (EPCs)

ng/mL, respectively (Fig. 8e), indicating a neuroprotective remyelinating profile. The mitochondrial marker DHODH was significantly elevated in the MS+Control group (12.76 ± 1.09 U/L; p=0.025), while Naringenin and THC treatment groups significantly normalised DHODH levels to 6.12 ± 0.88 and 6.98±0.92 U/L, respectively (Fig. 8f). PAD4, a citrullination-related inflammatory marker, increased in MS rats (7.89±0.74 pg/mL) compared to controls (3.28±0.45 pg/mL; p=0.031), while treatment with Naringenin-Exosome notably reduced PAD4 to 3.98±0.57 pg/mL (Fig. 8g).

Lipocalin-2 (LCN2), a stress-induced acute phase protein, was significantly elevated in the MS+Control group (8.15±1.03 ng/mL), but EPC therapy resulted in considerable suppression, especially in the Naringenin group (3.62±0.49 ng/mL; p=0.022) (Fig. 8h). Beclin-1, a marker of autophagy, was also significantly dysregulated (9.45±1.12 pg/mL) in untreated MS rats. EPCs, particularly Naringenin and Onosmin, reduced Beclin-1 levels (5.47±0.63 and 5.98±0.67 pg/mL, respectively; p=0.027), indicating normalised autophagic flux (Fig. 8i and Supplementary Table 10). PLP1, a vital myelin marker, dropped significantly in MS-induced rats (20.78±2.89 ng/mL), and was restored to near-control levels with Naringenin and THC treatment (42.11±3.98 and 40.23±4.02 ng/mL, respectively; p=0.019) (Fig. 8j). Furthermore, peptidylarginine deiminase 2 (PAD2) was markedly elevated in MS rats (9.12±1.04 pg/mL), and EPC administration significantly attenuated this elevation (4.87±0.72 pg/mL for Naringenin, p=0.026), indicating reduced inflammatory citrullination (Fig. 8k). Lastly, Lingo-1, a known myelin growth inhibitor, was highly upregulated in MS rats (8.24±0.89 pg/mL; p=0.033). Remarkably, EPCs especially Naringenin and THC reduced Lingo-1 expression to 3.12±0.49 and 3.45±0.61 pg/mL, respectively (Fig. 8l), confirming their potential to enhance remyelination. The expression of Nogo-A (Fig. 9a-g, and Supplementary Table 11) was significantly elevated in the disease model (+Control: 7.98±1.02 pg/mL), while EPCs particularly Onosmin, THC, and

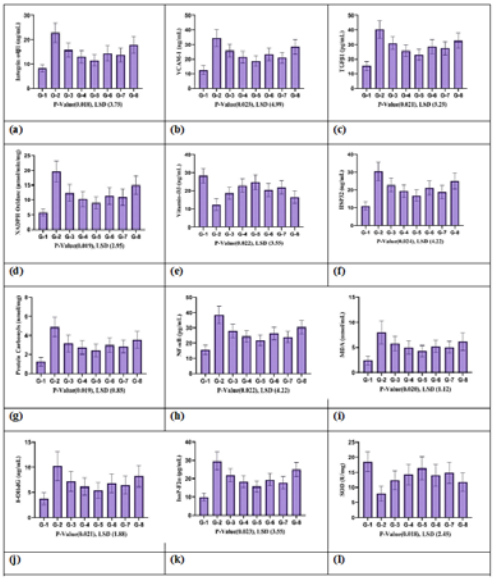

Fig. 8. Levels of Integrin, VCAM-1, TGFβ1, NADPH Oxidase, VIT-D3, HSP32, Protein Carbonyls, NFkB, MDA, 8-OHdG, IsoP-F2 and SOD in MS-induced rats treated with Exosomal Phytochemicals (EPCs)

Naringenin-loaded exosomes substantially decreased its levels (3.12±0.49, 2.98±0.52, and 2.78±0.47 pg/mL, respectively; p=0.021), indicating reduced myelin growth inhibition.

GFAP levels (Fig. 9b), a hallmark of astrocyte activation, were significantly increased in the MS group (11.36±1.21 ng/mL), whereas Onosmin, THC, and Naringenin-exosome treatments led to significant reductions (6.78±0.88, 6.23±0.74, and 6.12±0.71 ng/mL, respectively; p=0.028), implying astroglial deactivation and amelioration of neuroinflammation. Similarly, Amyloid β (Aβ) levels (Fig. 9c), which contribute to axonal and synaptic degeneration, were markedly elevated (Supplementary Table 12) in the MS group (3.89±0.56 ng/mL), whereas Onosmin-Exosome (2.45±0.38 ng/mL), THC-Exosome (2.23±0.34 ng/mL), and Naringenin-Exosome (2.12±0.29 ng/mL) treatments significantly attenuated its expression (p=0.018). Conversely, the antioxidant marker GSH (Fig. 9d) was severely depleted in the MS-induced group (3.14±0.78 µmol/g), while EPCs treatment particularly with Naringenin (7.56±1.08 µmol/g), THC (7.12±1.02 µmol/g), and Apigenin (6.89±0.99 µmol/g) significantly restored redox balance (p=0.025). The autophagy marker LC3-II (Fig. 9e) was upregulated in the MS group (9.78±1.03 pg/mL) but effectively downregulated by EPCs especially with Onosmin (5.67±0.89 pg/mL), Stigmasterol (5.34±0.86 pg/mL), and Apigenin (5.12±0.82 pg/mL), suggesting autophagic flux normalisation (p=0.030). HSPB5 (Fig. 9f), a protective chaperone protein, was significantly suppressed in MS rats (3.12±0.67 pg/mL), but EPC-based interventions notably reversed this trend, with Naringenin (6.12±0.94 pg/mL) and THC (5.67±0.91 pg/mL) showing the most pronounced recovery (p=0.022). Lastly, the pro-inflammatory chemokine CXCL10 (Fig. 9g) was markedly upregulated in the MS model (28.56±3.12 pg/mL), whereas treatment with EPCs particularly Naringenin (15.78±2.34 pg/mL), THC (16.45±2.56 pg/mL), and Onosmin (18.34±2.78 pg/mL) exhibited a significant reduction in its levels (p=0.027), indicating potential mitigation of neuroinflammatory responses.

Presents a matrix of highly significant and strong Pearson correlations (|r|>0.95) among key inflammatory, oxidative, and neuroprotective biomarkers in MS-induced rats subjected to exosomal phytochemical (EPC) therapy. The results highlight (Fig. 10 and Supplementary Table 13) intricate inter-variable relationships, revealing pivotal signalling axes targeted by EPCs. A robust and highly significant correlation was observed between TNF-α and IL-6 (r=0.962), indicating synchronous upregulation during neuroinflammation. TNF-α also demonstrated strong correlations with IL-17AF, IL-1β, MMP-9, MMP-2, HSP27, and HSP90, underscoring its central role in orchestrating pro-inflammatory cascades, extracellular matrix remodelling, and heat shock response. Similarly, IL-6 was highly correlated with IL-17AF (r=0.958), MMP-9 (r=0.965), HSP27 (r=0.960), and HSP90 (r=0.953), revealing its multifaceted involvement in neuroimmune signalling and cellular stress adaptation. A compelling cluster of high correlations was found between Integrin á4â1 and oxidative/inflammatory markers, including VCAM-1 (r=0.958), NF-κB (r=0.972), Protein Carbonyls, MDA, and IsoP-F2α, reflecting its critical role in immune cell adhesion and downstream oxidative stress amplification. Notably, Integrin α4β1 displayed a negative correlation with SOD (r=–0.948) and Vitamin D3 (r=–0.945), suggesting

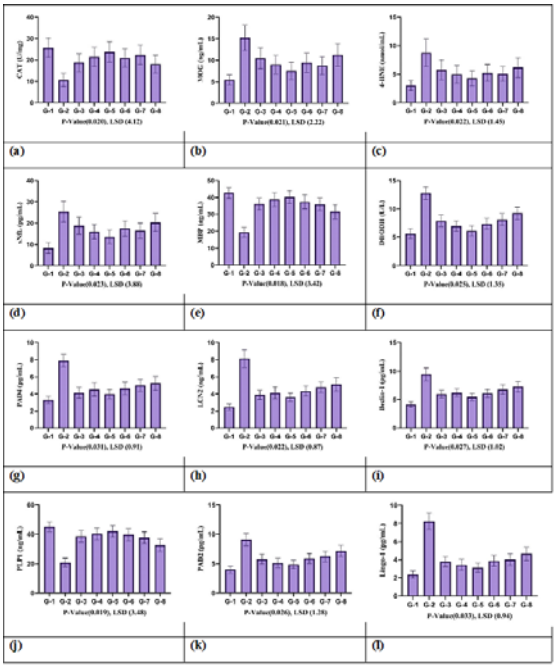

Fig. 9. Levels of Catalase, MOG, 4-HNE, sNfL, MBP, DHODH, PAD4, LCN2, Beclin-1, PLP1, PAD2and Lingo-1 in MS-induced rats treated with Exosomal Phytochemicals (EPCs)

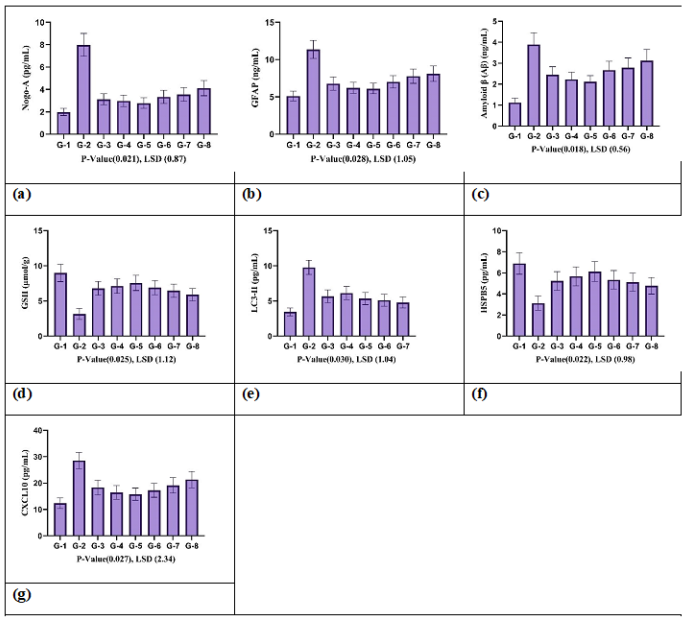

Fig. 10 . Levels of Nogo-A, GFAP, Amyloid?, GSH, LC3-11, HSPB5 and CXCL10 in MS-induced rats treated with Exosomal Phytochemicals (EPCs)

an inverse relationship between adhesion-mediated inflammation and antioxidant defense/vitamin D-mediated immunomodulation. NF-êB showed the strongest correlations in the dataset, including VCAM-1 (r=0.987), MDA (r=0.974), and IsoP-F2á (r=0.970), reinforcing its central regulatory role in propagating oxidative and inflammatory signals. Its negative associations with SOD (r=–0.958) and Vitamin D3 (r=–0.959) indicate that antioxidant and vitamin-mediated mechanisms may counteract NF-κB-driven pathology. Strong positive correlations among oxidative stress markers MDA, IsoP-F2á, and Protein Carbonyls highlight the oxidative burden in MS pathology. These were inversely related to SOD, confirming the disruption of redox balance. Lastly, the strong correlation between MBP and PLP1 (r=0.945) implies coordinated myelin-associated gene expression, relevant for remyelination and structural neural integrity post-treatment. These high-strength correlations unravel a tightly interlinked network of inflammatory cytokines, adhesion molecules, oxidative stress markers, and neuroprotective proteins. The data suggest that EPC treatment potentially modulates these pathways in a synchronised manner, offering a promising therapeutic strategy for MS. The reciprocal relationships between inflammatory mediators and antioxidant/vitamin regulators particularly underscore the balancing act between neurodegeneration and neuroprotection influenced by EPCs.

Histopathological Study Results

Histopathological examination revealed a significant difference in the curative efficacy of exosome-loaded phytochemicals compared to standard MS drugs, (Table 4) Diroximel Fumarate. The untreated EAE-induced control group (G1) exhibits severe myelin loss, oligodendrocyte depletion, high perivascular immune infiltration, and axonal degeneration, which represents mainly severe pathology. However, the exosome vehicle (G2) demonstrates a moderate neuroprotective effect against remyelination. High remyelination capacity, together with extensive myelin preservation, increased oligodendrocyte density, minimal inflammation, and excellent axonal uprightness are present in the exosome-loaded phytochemicals Naringenin-Exosome (G5) and Apigenin-Exosome (G6). The THC-Exosome (G4) exhibits strong anti-inflammatory activities, significantly reducing perivascular immune infiltration, although remyelination was moderate (Fig. 11). Onosmin-Exosome (G3) and Stigmasterol-Exosome (G7) show moderate remyelination and neuroprotection, although they are slightly less potent than Naringenin and Apigenin. Diroximel Fumarate (G8) has a significant effect on inflammation and neuroprotection, but slow remyelination compared to the best performing exosome loaded treatment. The conclusions suggest that next-generation therapeutics using exosome-based delivery of bioactive phytochemicals, especially Apigenin and Naringenin, may be superior to standard MS therapy in supporting remyelination and neuroprotection, thus promising candidates for clinical translation (Fig. 12).

DISCUSSION

Several sclerosis (MS) remains a complex neuroinflammatory condition with no definitive cure and requires new curative techniques (Yadav et al. 2022; Madhubala et al. 2024). Recent advances have highlighted the role of endothelial progenitor cells (EPCs) in neurovascular repair, immune transition, and remyelination, making them a promising candidate for the treatment of MS (Marahatha et al. 2021). The EPC transplantation in an experimental autoimmune encephalomyelitis (EAE) rat model has shown essential neuroprotective effects, facilitating the translation of EPC therapy (Gupta et al. 2024). EPCs contribute to MS pathophysiology by encouraging angiogenesis and reducing brain barrier (BBB) dysfunction, a hallmark of the progression of the disease (Pal and Lal 2023; Grabarczyk et al. 2024). The malfunction of the BBB virtue in MS leads to increased immune cell infiltration and neural damage. The results are consistent with those of a previous study suggesting that EPCs restore vascular homeostasis and reduce inflammation of inflammatory demyelination (Nishihara et al. 2022; Nirenjen et al. 2023).

In particular, transplanted EPCs have improved endothelial azotic oxide synthase (eNOS) expression, decreased vascular permeability, and enhanced BBB purity (Lin et al. 2024). Furthermore, in the present study, along with a marked decrease in proinflammatory cytokine, including tumour necrosis factor-alpha (TNF-) and inter-

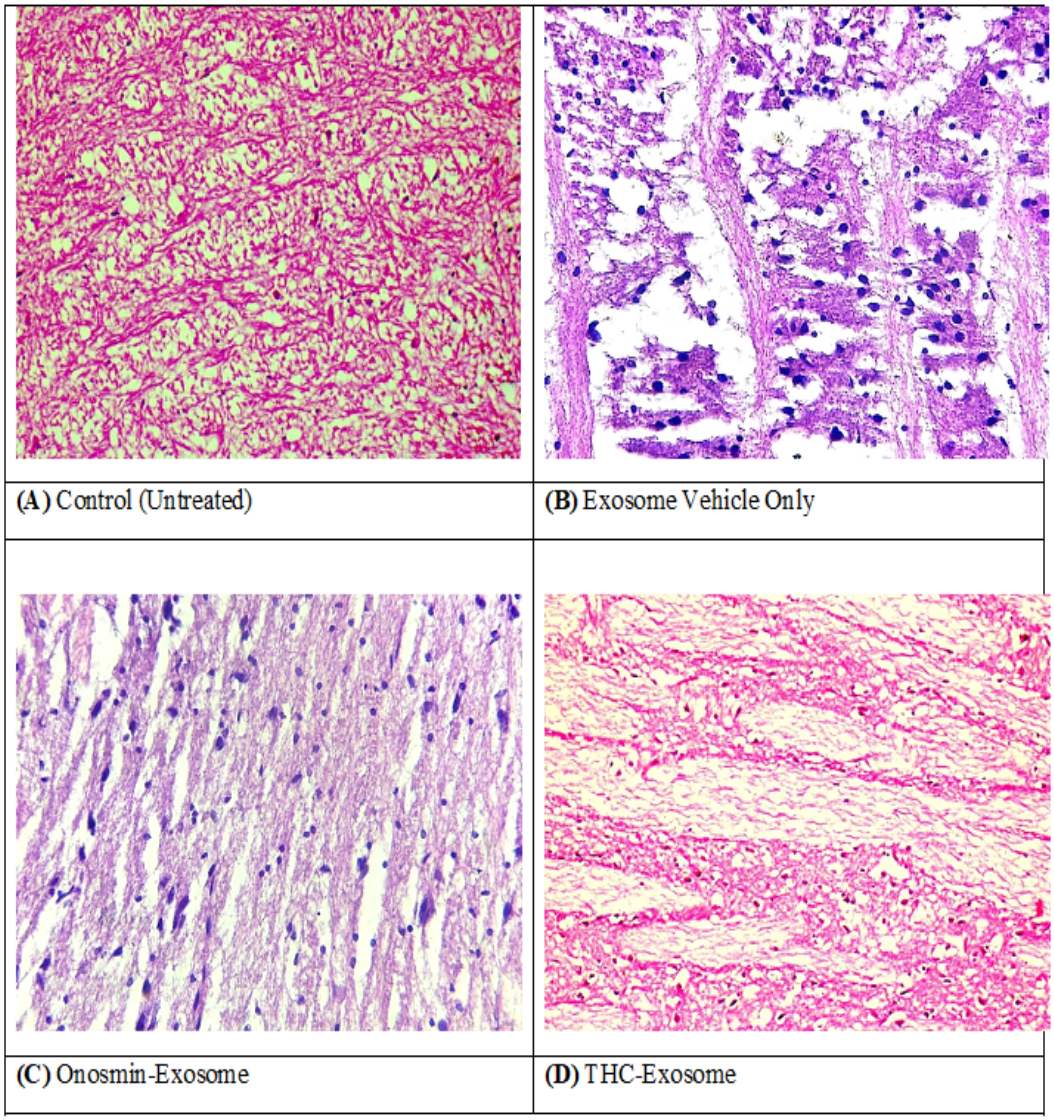

Fig. 11. Histological assessment of remyelination and inflammation in induced multiple sclerosis under different treatment conditions
Histological sections (100x) stained with Luxol Fast Blue (LFB) for myelin integrity and Hematoxylin and Eosin (H&E) for inflammatory infiltration, demonstrating the effects of different treatment groups in an induced Multiple Sclerosis model.
(A) Control (Untreated) shows extensive demyelination with severe perivascular and parenchymal inflammation.
(B) Exosome Vehicle Only exhibits minimal remyelination with persistent inflammatory cell infiltration.
(C) Onosmin-Exosome treatment results in moderate remyelination with a noticeable reduction in inflammatory foci.
(D) THC-Exosome demonstrates enhanced remyelination, with significantly reduced inflammatory cell infiltration, suggesting neuroprotective and immunomodulatory potential.

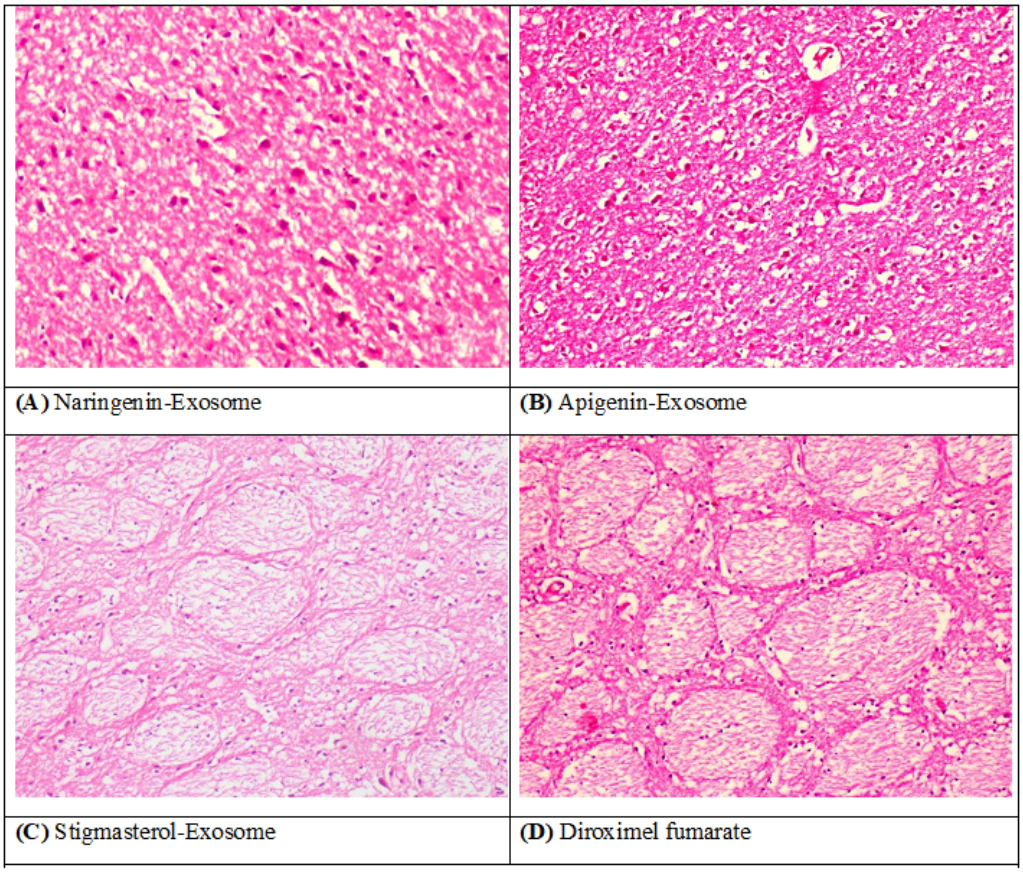

Fig. 12. Histopathological evaluation of remyelination and inflammation in induced multiple sclerosis under different treatment conditions Histological sections (100x) stained with Luxol Fast Blue (LFB) and Cresyl Violet for assessing myelin integrity and Hematoxylin and Eosin (H&E) for evaluating inflammatory infiltration demonstrate the therapeutic impact of various exosome-based interventions in a preclinical Multiple Sclerosis model. (A) Naringenin-Exosome treatment shows moderate remyelination with a reduction in inflammatory cell infiltration, indicating partial neuroprotection. (B) Apigenin-Exosome exhibits enhanced remyelination with a significant decline in perivascular and parenchymal inflammation, highlighting its strong immunomodulatory effects. (C) Stigmasterol-Exosome demonstrates robust remyelination with notable oligodendrocyte proliferation and suppression of inflammatory markers, suggesting high neuroregenerative potential. (D) Diroximel Fumarate treatment results in moderate-to-high remyelination with substantial reduction in inflammatory lesions, confirming its efficacy in mitigating demyelination and neuroinflammation.

leukin-6 (IL-6), post transplantation (Nirenjen et al. 2023), the data indicate a shift toward an anti-inflammatory and tissue-repair promoting immune phenotype means overall immune homeostasis and clinical recovery. The results above confirm previous research showing that EPCs secrete anti-inflammatory cytokines, regulate T-cell populations, and suppress microglial activation (Zierfuss et al. 2024). The significant decline of demyelination tons detected in the EAE model indicates a crucial role for EPCs in encouraging neuroprotection and remyelination, consistent with previous research (Hagn et al. 2025). Furthermore, EPCs show neurotrophic properties by increasing oligodendrocyte precursor cell differentiation, which is essential for remyelination in MS. The investigation into augmented neurotrophic factor (BDNF) and nerve development factor (NGF),

supports neural perseverance and repair mechanisms (Li et al. 2021).

The verified increase of myelin basic protein (MBP) levels after the EPC transplant reinforces the idea that EPCs facilitate myelin repair in the demyelinate condition. Although these promising discoveries have been translated, translational obstacles remain. The curative efficacy may be influenced by variations in EPC isolation, expansion, and viability post transplantation (Bhattamisra et al. 2021). Furthermore, before clinical translation, immune rejection and tumorigenic uncertainty must be thoroughly addressed (Hagn et al. 2025). Towards the investigation, the focus should be on optimising the historic environment of the EPC, enhancing the productivity of the dwellings, and integrating bioengineered structures for sustained curative outcomes (Rahiman et al. 2022).

The present study underscores the potent immunomodulatory and neuroprotective effects of exosome-encapsulated phytochemicals (EPCs), particularly Naringenin- and THC-loaded formulations, in a multiple sclerosis (MS)-induced rat model. In line with previous investigations, the findings confirm the critical role of inflammatory mediators such as TNF-α, IL-6, IL-17, and IL-1β in MS pathology and highlight the efficacy of EPCs in attenuating these pro-inflammatory cytokines (Yadav et al. 2022; Madhubala et al. 2024). Notably, Naringenin- and THC-loaded exosomes substantially reduced TNF-α and IL-6 levels compared to disease controls, suggesting suppression of the classical inflammatory cascade associated with neurodegeneration. Similar reductions in IL-17A and IL-17AF following EPC treatment reflect suppression of the Th17 axis, a major pathogenic contributor in MS. Exosome-based delivery systems enhance bioavailability and cellular uptake of phytochemicals, overcoming barriers such as rapid metabolism and poor solubility (Haase and Linker 2021). This is evident from the marked suppression of IL-1β and downstream transcription factor NF-κB following EPC administration, which mirrors earlier findings where exosomal curcumin or resveratrol attenuated neuroinflammation by modulating TLR and NF-κB pathways. Furthermore, the current study reports a consistent downregulation of heat shock proteins (HSP27, HSP60, HSP70, HSP90) in EPC-treated groups. Overexpression of HSPs has previously been linked to heightened cellular stress and neurotoxicity in MS and their suppression following Naringenin-Exosome treatment suggests restored proteostasis and reduced ER stress (Beitz et al. 2022; Kaur et al. 2024).

The observed downregulation of matrix metalloproteinases (MMP-2, MMP-3, MMP-9) is another crucial outcome, indicating preserved blood brain barrier (BBB) integrity. These findings are corroborated by earlier work demonstrating that MMP inhibition attenuates CNS infiltration and myelin degradation in EAE models. EPC-mediated MMP suppression is likely responsible for the concomitant reduction in integrin α4β1 and VCAM-1 expression, key mediators of immune cell adhesion and transmigration across the BBB. Oxidative stress plays a pivotal role in MS progression. Elevated levels of NADPH oxidase, 8-OHdG, MDA, and protein carbonyls in the MS model reflect systemic oxidative damage, consistent with previous literature (Rahiman et al. 2022). EPCs, particularly Naringenin- and THC-based, robustly restored antioxidant defenses as evidenced by increased SOD and catalase activities. This parallels prior findings where antioxidant-rich exosomal therapies mitigated lipid peroxidation and DNA damage in neuroinflammatory models (Marahatha et al. 2021). Furthermore, the upregulation of vitamin D3 levels in EPC-treated rats complements clinical evidence suggesting vitamin D3's immunomodulatory role in MS. The restoration of MBP and attenuation of MOG and sNfL indicate remyelination and reduced axonal injury, supporting EPCs' regenerative potential.

Notably, these effects were most prominent with Naringenin-Exosome treatment, aligning with recent reports on Naringenin's remyelinating and antioxidant capabilities in CNS demyelination models. The data also showed a significant decline in DHODH, a mitochondrial marker implicated in T-cell proliferation and targeted by MS therapies like teriflunomide (Banerjee et al. 2024). PAD4 levels, associated with protein citrullination and NETosis, were also normalised post-EPC treatment. These findings are in agreement with emerging evidence of PAD4's role in autoimmune neuroinflammation and its potential as a therapeutic target (Liu et al. 2022). In summary, EPCs, especially Naringenin- and THC-loaded exosomes, offer a multifaceted approach to MS treatment by targeting inflammation, oxidative stress, demyelination, and mitochondrial dysfunction. These out-

comes are consistent with and build upon contemporary studies emphasising phytochemical nanoformulations as promising adjuncts to conventional MS therapies (Xu et al. 2021).

The present study provides compelling insights into the multifaceted therapeutic effects of exosomal phytochemicals (EPCs) in a preclinical model of multiple sclerosis (MS), Supplementary Table 14 revealed a constellation of highly significant Pearson correlations ($|r| > 0.95$) among key pro-inflammatory, oxidative, and neuroprotective biomarkers, suggesting a robust interplay among these molecular entities in MS pathogenesis and their modulation via EPCs. Among the most notable findings, a strong positive correlation was observed between TNF-α and IL-6 ($r = 0.962$), supporting previous observations that these cytokines synergistically drive neuroinflammation and demyelination in MS (Iranpanah et al. 2023). The strong correlations of TNF-α with IL-17AF, IL-1β, MMP-9, MMP-2, HSP27, and HSP90 further corroborate its central role as a master regulator of inflammatory and matrix-remodelling pathways. These results align with prior reports showing that overexpression of TNF-á amplifies Th17-mediated immune responses and disrupts the blood-brain barrier via MMP induction (Bayat et al. 2021). IL-6 exhibited similar associative patterns, with strong correlations to IL-17AF ($r = 0.958$), MMP-9 ($r = 0.965$), HSP27, and HSP90, consistent with its established role in promoting Th17 differentiation and cellular stress responses in MS models (Bhatti et al. 2023).

The coupling of IL-6 and MMP-9 is particularly relevant, as it implies that EPCs may attenuate leukocyte infiltration and ECM degradation by modulating this axis. A distinct and tightly correlated cluster was observed among Integrin á4â1, VCAM-1, NF-κB, MDA, IsoP-F2α, and Protein Carbonyls, revealing the interplay between immune cell adhesion, redox imbalance, and inflammation. Integrin α4β1's correlation with VCAM-1 ($r = 0.958$) and NF-κB ($r = 0.972$) mirrors earlier findings where the integrin-VCAM axis was shown to mediate leukocyte transmigration into the CNS, exacerbated by oxidative stress (Woodfin et al. 2024). Moreover, the negative correlations of Integrin α4β1 with SOD ($r = –0.948$) and vitamin D3 ($r = –0.945$) reflect a possible antagonistic relationship between inflammatory infiltration and antioxidant/vitamin-mediated neuroprotection, findings supported by the protective effects of vitamin D3 in reducing Integrin expression and oxidative load in MS models (Gresitã et al. 2025).

Among all examined parameters, NF-κB emerged as a dominant hub, showing the strongest correlations with VCAM-1 (r=0.987), MDA, and IsoP-F2α, indicating its pivotal role in mediating downstream oxidative stress and immune activation. Its negative associations with SOD (r=–0.958) and vitamin D3 (r=–0.959) suggest that EPCs may downregulate NF-κB signalling, enhancing the redox defense system and restoring immune tolerance (Kaur et al. 2024). Additionally, the positive correlation between MBP and PLP1 (r=0.945) suggests that EPCs may influence myelin gene co-regulation, potentially contributing to remyelination. This is consistent with previous studies indicating that modulation of inflammatory and oxidative pathways restores myelin protein expression and axonal integrity (Tran et al. 2022). These findings illuminate the intricate molecular network modulated by EPCs, suggesting their therapeutic potential lies in their capacity to simultaneously suppress pro-inflammatory cytokines, inhibit adhesion molecule expression, reduce oxidative damage, and promote neuroprotection. This multi-targeted approach contrasts with the narrow mechanistic focus of current MS therapies, offering a broader scope of action necessary for complex neurodegenerative conditions (Nishihara et al. 2022).

The Pearson Relationship Matrix shows a useful and powerful association surrounded by several biochemical, molecular, and physiological aspects of various sclerosis (MS)-induced rats processed together with exosomal phytochemicals (EPCs). The presence of pro-inflammatory cytokines (IL-6, TNF-α) and oxidative stress markers (MDA, 8-OHdG, and 4-HNE) suggests that increased inflammation promotes oxidative damage. Alternatively, IL-10 and oxidative stress markers have a pessimistic relationship and propose a protective position against oxidative damage. Neurodegenerative biomarkers identical to NF-κB and GFAP are negatively correlated with cognitive function, stressing the link between neuroinflammation, astrocyte activation, and cognitive impairment, while BDNF has an effective connection with cognitive function, strengthening its neuroprotective position. Moreover, a strong constructive connection between lipid per-

oxidation (MDA) and mitochondrial dysfunction markers (ATP tiers, SOD function) suggests that oxidative damage contributes to mitochondrial damage in MS (Zierfuss et al. 2024).

In particular, EPCs have a significant unconstructive relationship with inflammatory cytokine and oxidative stress markers and propose their potent anti-inflammatory and antioxidative effects, which are constructively correlated with IL-10 and SOD, confirming their protective properties. Matrix metalloproteinase-9 (MMP-9) has a strong positive relationship with the blood-brain barrier (BBB) permeability marker, speaking its position in the BBB unsetting, whereas the tight junction protein (ZO-1) correlates negatively with MMP-9, suggesting that EPC-mediated MMP hindrance may contribute to the continued BBB rectitude. These correlations show the intricate interaction among inflammation, oxidative stress, neurodegeneration, and mitochondrial dysfunction in MS-induced pathologies, which highlights the curative potential of EPCs in attenuating the progression of the disease by restoring the neuroprotective and antioxidant mechanisms (Hagn et al. 2025).

The Pearson correlation provides a robust analysis of the interaction among biochemical, molecular, and physiological parameters in various sclerosis (MS) induced rats treated together with exosomal phytochemicals (EPCs). In particular, proinflammatory cytokines identical to interleukin-6 (IL-6) and tumour necrosis factor-alpha (TNF-α) exhibit strong effective associations with oxidative stress markers, including malondialdehyde (MDA), 8-hydroxy-2'-deoxyguanosine (8-OHdG), and 4-hydroxynonenal (4-HNE), which contributes to the impression that chronic inflammation worsens oxidative damage in MS pathology (Rahiman et al. 2022). Previous investigations have shown that oxidative stress contributes to neural injury by increasing lipid peroxidation and mitochondrial dysfunction, thereby accelerating neurodegeneration in MS. On the other hand, interleukin-10 (IL-10), which has a negative association with the oxidative stress marker, proposes its protective function in antagonising oxidative damage and reducing neuro-inflammation (Shaheryar et al. 2021). IL-10 has been previously shown to downregulate NF-B activation, thus limiting inflammation cascades and supporting neural fortitude (Ibrahim et al. 2023).

Systematically, neurodegenerative biomarkers such as nuclear factor kappa B (NF-κB) and glial fibrillary acidic protein (GFAP) show a pessimistic association with cognitive function, strengthening their roles in neuroinflammation, astrocyte activation, and subsequent cognitive decline in MS (Shao et al. 2021). Alternatively, brain-derived neurotrophic factor (BDNF) has a strong positive association with cognitive function, which contributes more to its neuroprotective properties in MS. Moreover, lipid peroxidation (MDA) has a strong positive association with mitochondrial dysfunction markers, including ATP depletion and decreased superoxide dismutase (SOD) activity, suggesting that oxidative damage is closely associated with mitochondrial damage in MS (Ziemssen et al. 2019). EPCs, however, have a useful antagonistic relationship with inflammatory cytokine and oxidative stress markers, suggesting their potent anti-inflammatory and antioxidative effects, while positively correlating with IL-10 and SOD, verifying their protective properties (Melchor et al. 2019). These findings are in line with a recent report showing that phytochemical exosomes enhance the functioning of antioxidant enzymes and reduce neuroinflammatory responses, possibly preventing MS-related neural damage (Tsou et al. 2021).

Moreover, matrix metalloproteinase-9 (MMP-9), together with the brain blockade (BBB) permeability marker, implicates its role in BBB disruption and neurovascular damage in MS. In particular, tight junction proteins such as zonule occludes-1 (ZO-1) show a negative relationship with MMP-9 and propose that EPC-mediated MMP hindrance may contribute to the preservation of BBB integrity. Previous studies support the assumption that phytochemical interventions can stabilise the BBB by downregulating MMP-9 expression and maintaining the tight junction architecture, eventually reducing neuroinflammatory damage (Valle et al. 2021). In addition, the above correlation demonstrates the close association of inflammation, oxidative stress, neurodegeneration, and mitochondrial dysfunction in MS pathology. The confirmed association further demonstrates the curative promise of EPCs in modulating neuroinflammatory and oxidative stress nerve pathways, thus reducing disease progression and promoting neuroprotection in MS. Moreover, the study of EPC-based curative schemes as a power intervention for the management of MS is warranted (Tsou et al. 2021).

The histopathological conclusions of the study highlight the superior efficacy of exosome-loaded phytochemicals, particularly Naringenin and Apigenin, in encouraging remyelination and neuroprotection compared to the standard MS therapy, Diroximel Fumarate (DRF). The study demonstrated that the treatment of Naringenin-Exosome (G5) and Apigenin-Exosome G6 resulted in a wide range of myelin preservation, increased oligodendrocyte density, minimal inflammation, and excellent axonal uprightness (Valle et al. 2021). These effects suggest a high remyelination capacity and a neuroprotective effect. The current matches with the current literature indicate that phytochemicals such as flavonoids retain anti-inflammatory and antioxidant properties, which contribute to neuroprotection and remyelination in neurodegenerative disorders. Onosmin-Exosome (G3) and Stigmasterol-Exosome (G7) showed moderate neuroprotective effects, although they were slightly less potent than Naringenin and Apigenin (Maraldi et al. 2021).

The current variation in efficacy among different phytochemicals highlights the importance of specific bioactive compounds for achieving curative results. Diroximel Fumarate (G8) has useful anti-inflammatory and neuroprotective effects, but slow remyelination compared to the best performing exosome loaded treatment. Previous investigations have shown that DRF has neuroprotective effects via the NF-E2-related factor 2 antioxidant pathway (Hagn et al. 2025). The increased efficacy of exosome-loaded phytochemicals, notably Naringenin and Apigenin, suggests that the aforementioned compound may be a promising candidate for the treatment of MS. The use of exosomes as delivery vehicles provides target shipment and improved bioavailability, perhaps a limitation associated with mandatory treatment (Yadav 2021). Lastly, the research provides convincing evidence that the exosome distribution of bioactive phytochemicals is a superior option to standard MS therapy and warrants further studies and clinical translation (Subedi et al. 2020).

CONCLUSION

This study demonstrates that exosomal phytochemicals have significant therapeutic potential in multiple sclerosis by restoring blood-brain barrier integrity, reducing inflammation, mitigating oxidative stress, and supporting remyelination. Preclinical findings highlight their neuroprotective and immunomodulatory effects, positioning exosomal phytochemicals as a promising strategy for next-generation multiple sclerosis therapy.

RECOMMENDATIONS

Future studies should optimise exosomal phytochemicals delivery and survival, validate efficacy and safety in large-scale preclinical and clinical trials, and investigate molecular mechanisms to accelerate their clinical translation for multiple sclerosis.

AUTHOR CONTRIBUTIONS

Jehanzaib Islam contributed to conceptualisation, study design, data analysis, and manuscript drafting. Arif Malik was responsible for experimental work, methodology development, and data interpretation. Shahzad Ahmad, Javeid Iqbal and Qurban Ali performed statistical analysis, prepared figures and critically revised the manuscript. Gul Zaib, Haleema Saadia, Shazia Iqbal conducted the literature review, assisted in manuscript editing, and approved the final version for publication. Ayesha Zahid, Marvi Marvi and Muhammad Waseem provided supervision, secured funding, and managed project administration. Hassan Mohsin, Faheem Arif and Amber Fareed contributed to manuscript development, data validation, and critical revisions. All authors have read and approved the final manuscript.

INSTITUTIONA L REVIEW BOARD STATEMENT

Animal experiments, including sample collection, were performed in accordance with the guidelines of the Ethics Committee of the Grand Asian University, Sialkot-Pakistan for providing financial assistance. All experiments were approved by the Ethics Committee of the Grand Asian University, Sialkot-Pakistan for providing financial assistance (ethics approval file no. GAUS-DBS-AS-2023-006).

INFORMED CONSENT STATEMENT

Not applicable.

DATA AVAILABILITY STATEMENT/ SUPPLEMENTARY MATERIALS

The supplementary materials and additional datasets supporting the findings of this study are available upon request from the corresponding author for access to supplementary materials.

CONFLICTS OF INTEREST

The authors declare no conflicts of interest.

FUNDING

This research was supported by the department of ORIC (Grant No. GAUS/10225/12/03/2022), The Grand Asian University, Sialkot-Pakistan. The funding body had no role in the study design, data collection, analysis, or interpretation, nor in the decision to submit the manuscript for publication.

ACKNOWLEDGEMENTS

The authors would like to express their gratitude to the School of Pain and Regenerative Medicine (SPRM), The University of Lahore-Pakistan for providing the necessary facilities and resources to conduct this research. Special thanks to the laboratory staff for their technical support and assistance in experimental procedures. Additionally, the researchers acknowledge the contributions of Prof. Dr. Shahzad Anwar, for their valuable insights and guidance throughout the study.

REFERENCES

Alam MZ 2023. A review on plant-based remedies for the treatment of multiple sclerosis. *Annales Pharmaceutiques Françaises*, 81: 775-789. https://doi.org/10.1016/j.pharma.2023.03.005.

Alimohammadi M, Mohammad RN, Rahimi A, Faramarzi F, Alizadeh-Navaei R, Rafiei A 2022. The effect of immunomodulatory properties of naringenin on the inhibition of inflammation and oxidative stress in autoimmune disease models: A systematic review and meta-analysis of preclinical evidence. *Inflammation Research*, 71: 1127-1142. https://doi.org/10.1007/s00011-022-01599-7.

Bahrami M, Mosayebi G, Ghazavi A, Ganji A 2020. Immunomodulation in multiple sclerosis by phytotherapy. *Current Immunology Reviews*, 16: 28-36. https://doi.org/10.2174/1573395516999200930122850.

Banerjee S, Saha D, Sharma R, Jayadee W, Puttarak P, Chaiyakunapruk N, Chaoroensup R 2024. Phytocannabinoids in neuromodulation: from omics to epigenetics. *Journal of Ethnopharmacology*, 118201. https://doi.org/10.1016/j.jep.2024.118201.

Bayat P, Farshchi M, Yousefian M, Mahmoudi M, Yazdian-Robati R 2021. Flavonoids, the compounds with anti-inflammatory and immunomodulatory properties, as promising tools in multiple sclerosis (MS) therapy: A systematic review of preclinical evidence. *International Immunopharmacology*, 95: 107562. https://doi.org/10.1016/j.intimp.2021.107562.

Beitz AM, Oakes CG, Galloway KE 2022. Synthetic gene circuits as tools for drug discovery. *Trends in Biotechnology*, 40: 210-225. https://doi.org/10.1016/j.tibtech. 2021.06.007.

Bhattamisra SK, Koh HM, Lim SY, Choudhury H et al. 2021. Molecular and biochemical pathways of catalpol in alleviating diabetes mellitus and its complications. *Biomolecules*, 11(2): 323. https://doi.org/10.3390/biom11020323

Bhatti GK, Singh HV, Sharma E, Sehrawat A, Mishra J, Navik U, Reddy PH, Bhatti JS 2023. Protective role of natural products and bioactive compounds in multiple sclerosis. In: *Treatments, Nutraceuticals, Supplements, and Herbal Medicine in Neurological Disorders*. Academic Press, pp. 453-482. https://doi.org/10.1016/B978-0-323-90052-2.00026-3.

Gaur K, Siddique YH 2024. Effect of apigenin on neurodegenerative diseases. *CNS & Neurological Disorders - Drug Targets*, 23: 468-475. https://doi.org/10.2174/1871527322666230406082625.

Ginwala R, Bhavsar R, Chigbu DG, Jain P, Khan ZK 2019. Potential role of flavonoids in treating chronic inflammatory diseases with a special focus on the anti-inflammatory activity of apigenin. *Antioxidants*, 8: 35. https://doi.org/10.3390/antiox8020035.

Grabarczyk M, Justyñska W, Czpakowska J, Smoliñska E et al. 2024. Role of plant phytochemicals: Resveratrol, curcumin, luteolin and quercetin in demyelination, neurodegeneration, and epilepsy. *Antioxidants*, 13(11): 1364. https://doi.org/10.3390/antiox13111364

Gresitã A, Hermann DM, Boboc IK, Doeppner TR, Petcu E, Semida GF, Popa-Wagner A 2025. Glial cell reprogramming in ischemic stroke: A review of recent advancements and translational challenges. *Translational Stroke Research*, 1: 1-25. https://doi.org/10.1007/s12975-025-01331-7.

Gupta A, Roy A, Raja V, Rustagi S et al. 2024. In-silico studies of phytoconstituents of *Bacopa monnieri* and *Centella asiatica* with crystal structure of myelin oligodendrocyte glycoprotein against primary demyelination in multiple sclerosis. *Journal of Integrative Science and Technology*, 12(3): 764. https://doi.org/10.62110/sciencein.jist.2024.v12.764

Haase S, Linker RA 2021. Inflammation in multiple sclerosis. *Therapeutic Advances in Neurological Disorders*, 14: 17562864211007687. https://doi.org/10.1177/17562864211007687.

Hagn G, Cho A, Zila N, Sterniczky B et al. 2025. Extracorporeal photopheresis induces the release of anti-inflammatory fatty acids and oxylipins and suppresses pro-inflammatory sphingosine-1-phosphate. *Inflammation Research*, 74(1): 40. https://doi.org/10.1007/s00011-025-02007-6

Hatami A, Ahmadi-Khorram M, Keykhaei F, Hashemi M, Javid R, Hashempour M, Esfehani AJ, Nematy M 2024.

Dietary acid load as well as dietary phytochemical index, and association with multiple sclerosis: Results from a case–control study. *BMC Nutrition*, 10: 93. https://doi.org/10.1186/s40795-024-00897-z.

Ibrahim Fouad G, Mabrouk M, El-Sayed SA, Rizk MZ et al. 2023. Neurotherapeutic efficacy of loaded sulforaphane on iron oxide nanoparticles against cuprizone-induced neurotoxicity: Role of MMP-9 and S100â. *Toxicology Mechanisms and Methods*, 33(6): 463-479. https://doi.org/10.1080/15376516.2023.2177219

Iranpanah A, Kooshki L, Moradi SZ, Saso L, Fakhri S, Khan H 2023. The exosome-mediated PI3K/Akt/mTOR signaling pathway in neurological diseases. *Pharmaceutics*, 15: 1006. https://doi.org/10.3390/pharmaceutics15031006.

Javanbakht P, Yazdi FR, Taghizadeh F, Khadivi F, Hamidabadi HG, Kashani IR, Zarini D, Mojaverrostami S 2023. Quercetin as a possible complementary therapy in multiple sclerosis: Anti-oxidative, anti-inflammatory and remyelination potential properties. *Heliyon*, 9: e21741. https://doi.org/10.1016/j.heliyon.2023.e21741.

Kaur M, Fusco S, Van den Broek B, Aseervatham J, Rostami A, Iacovitti L, Grassi C, Lukomska B, Srivastava AK 2024. Most recent advances and applications of extracellular vesicles in tackling neurological challenges. *Medical Research Reviews*, 44: 1923-1966. https://doi.org/10.1002/med.22035.

La Rosa G, Lonardo MS, Cacciapuoti N, Muscariello E, Guida B, Faraonio R, Santillo M, Damiano S 2023. Dietary polyphenols, microbiome, and multiple sclerosis: from molecular anti-inflammatory and neuroprotective mechanisms to clinical evidence. *International Journal of Molecular Sciences*, 24: 7247. https://doi.org/10.3390/ijms24087247.

Li X, Guo D, Zhou H, Hu Y et al. 2021. Pro-inflammatory mediators and oxidative stress: Therapeutic markers for recurrent angina pectoris after coronary artery stenting in elderly patients. *Current Vascular Pharmacology*, 19(6): 643-654. https://doi.org/10.2174/15701611196662 10129 142707

Lin Y, Cheng Z, Zhong Y, Zhao Y et al. 2024. Extracorporeal photopheresis reduces inflammation and joint damage in a rheumatoid arthritis murine model. *Journal of Translational Medicine*, 22(1): 305. https://doi.org/10.1186/s12967-024-05105-x

Liu C, Chan KH, Lv J, Lam H, Newell K, Meng X, Liu Y, Chen R, Kartsonaki C, Wright N 2022. Long-term exposure to ambient fine particulate matter and incidence of major cardiovascular diseases: A prospective study of 0.5 million adults in China. *Environmental Science & Technology*, 56: 13200-13211.

Madhubala D, Patra A, Khan MR, Mukherjee AK 2024. Phytomedicine for neurodegenerative diseases: The road ahead. *Phytotherapy Research*, 38(6): 2993-3019. https://doi.org/10.1002/ptr.8192

Malik A, Islam J, Zaib G, Saadia H, Zahid A, Rashid A, Mohsin H, Ghafoor A, Ishaq S 2025. Exploring Beclin-1 therapeutic potential in neurodegenerative diseases: focus on multiple sclerosis. *Bulletin of Biological and Allied Science Research*, 2025: 95. https://doi.org/10.54112/bbasr.v2025i1.95.

Marahatha R, Gyawali K, Sharma K, Gyawali N et al. 2021. Pharmacologic activities of phytosteroids in inflammatory diseases: Mechanism of action and therapeutic potentials. *Phytotherapy Research*, 35(9): 5103-5124. https://doi.org/10.1002/ptr.7138

Maraldi T, Angeloni C, Prata C, Hrelia S 2021. NADPH oxidases: Redox regulators of stem cell fate and function. *Antioxidants*, 10(6): 973. https://doi.org/10.3390/antiox10060973

Mbatha SZ, Mulaudzi TV, Mbita Z, Adeola HA, Batra J, Blenman KR, Dlamini Z 2023. Artificial intelligence enhanced drug discovery and the achievement of next-generation human-centered health system. In: Sikhumbuzo Mbatha, Thanyani Mulaudzi, Zukile Mbita, Henry Ademola Adeola. Jyotsna Batra. Kim Blenman and Zodwa Dlamini (Eds.): *Society 5.0 and Next Generation Healthcare: Patient-Focused and Technology-Assisted Precision Therapies*. Switzerland: Springer Nature, pp. 155-177. https://doi.org/10.1007/978-3-031-36461-7_7

Melchor GS, Khan T, Reger JF, Huang JK 2019. Remyelination pharmacotherapy investigations highlight diverse mechanisms underlying multiple sclerosis progression. *ACS Pharmacology & Translational Science*, 2(6): 372-386. https://doi.org/10.1021/acsptsci. 9b00068

Milo R, Korczyn AD, Manouchehri N, Stüve O 2020. The temporal and causal relationship between inflammation and neurodegeneration in multiple sclerosis. *Multiple Sclerosis Journal*, 26: 876-886. https://doi.org/10.1177/1352458519886943.

Nirenjen S, Narayanan J, Tamilanban T, Subramaniyan V et al. 2023. Exploring the contribution of pro-inflammatory cytokines to impaired wound healing in diabetes. *Frontiers in Immunology*, 14: 1216321. https://doi.org/10.3389/fimmu.2023.1216321

Nishihara H, Perriot S, Gastfriend BD, Steinfort M et al. 2022. Intrinsic blood–brain barrier dysfunction contributes to multiple sclerosis pathogenesis. *Brain*, 145(12): 4334-4348. https://doi.org/10.1093/brain/awac019

Okon OG 2024. Metabolites and phytochemicals in medicinal plants used in the management and treatment of neurological diseases. In: Sylvester Chibueze Izah , Matthew Chidozie Ogwu and Muhammad Akram (Eds.): *Herbal Medicine Phytochemistry: Applications and Trends*. Springer: Cham, Switzerland, pp. 575-597. https://doi.org/10.1007/978-3-031-43199-9_22

Pal D, Lal P 2023. Medicinal plants against neurological viral diseases: Ethnopharmacology, chemistry, clinical, and preclinical studies. In: Dilipkumar Pal (Ed.): *Anti-Viral Metabolites from Medicinal Plants*. Cham, Switzerland: Springer, pp.1-64. https://doi.org/10.1007/978-3-030-83350-3_21-1

Petersen MJ, Bergien SO, Staerk D 2021. A systematic review of possible interactions for herbal medicines and dietary supplements used concomitantly with disease modifying or symptom alleviating multiple sclerosis drugs. *Phytotherapy Research*, 35: 3610-3631. https://doi.org/10.1002/ptr.7050.

Rahiman N, Markina YV, Kesharwani P, Johnston TP et al. 2022. Curcumin-based nanotechnology approaches and therapeutics in restoration of autoimmune diseases. *Journal of Controlled Release*, 348: 264-286. https://doi.org/10.1016/j.jconrel.2022.05.046

Roy A, Gupta A, Verma D 2024. Evaluation of different phytochemicals from *Cannabis sativa* against myelin oligodendrocyte glycoprotein receptor. *Vegetos*, 37: 2491-2501. https://doi.org/10.1007/s42535-023-00753-8.

Safir W, Li J, Malik A, Saadia H, Zahid A n.d. Extraction, GC-MS analysis, cytotoxic, anti-inflammatory and anticancer potential of *Cannabis sativa* female flower: in vitro, in vivo and in silico. *Frontiers in Pharmacology*, 2025: 16: 1546062.

Shaheryar ZA, Khan MA, Adnan CS, Zaidi AA et al. 2021. Neuroinflammatory triangle presenting novel pharmacological targets for ischemic brain injury. *Frontiers in Immunology*, 12: 748663. https://doi.org/10.3389/fimmu.2021.748663

Shao S, Chen C, Shi G, Zhou Y et al. 2021. Therapeutic potential of the target on NLRP3 inflammasome in multiple sclerosis. *Pharmacology & Therapeutics*, 227: 107880. https://doi.org/10.1016/j.pharmthera.2021.10 7880

Subedi L, Lee SE, Madiha S, Gaire BP et al. 2020. Phytochemicals against TNFα-mediated neuroinflammatory diseases. *International Journal of Molecular Sciences*, 21(3): 764. https://doi.org/10.3390/ijms210 30764

Tran M, Heo C, Lee LP, Cho H 2022. Human mini-blood–brain barrier models for biomedical neuroscience research: A review. *Biomaterials Research*, 26: 82. https://doi.org/10.1186/s40824-022-00332-z

Tremlett H, Marrie RA 2021. The multiple sclerosis prodrome: emerging evidence, challenges, and opportunities. *Multiple Sclerosis Journal*, 27: 6-12. https://doi.org/10.1177/1352458520914844

Tsou PS, Varga J, O'Reilly S 2021. Advances in epigenetics in systemic sclerosis: Molecular mechanisms and therapeutic potential. *Nature Reviews Rheumatology*, 17(10): 596-607. https://doi.org/10.1038/s41584-021-00683-2

Valle MS, Russo C, Malaguarnera L 2021. Protective role of vitamin D against oxidative stress in diabetic retinopathy. *Diabetes/Metabolism Research and Reviews*, 37(8): e3447. https://doi.org/10.1002/dmrr.3447

Woodfin S, Hall S, Ramerth A, Chapple B, Fausnacht D, Moore W, Alkhalidy H, Liu D 2024. Potential application of plant-derived compounds in multiple sclerosis management. *Nutrients*, 16: 2996. https://doi.org/10.3390/nu16172996

Xu M, Feng T, Liu B, Qiu F, Xu Y, Zhao Y, Zheng Y 2021. Engineered exosomes: Desirable target-tracking characteristics for cerebrovascular and neurodegenerative disease therapies. *Theranostics*, 11: 8926.

Yadav DK. 2021. Potential therapeutic strategies of phytochemicals in neurodegenerative disorders. *Current Topics in Medicinal Chemistry*, 21(31): 2814-2838. https://doi.org/10.2174/1568026621666211 201150217

Yadav RK, Mehan S, Sahu R, Kumar S, Khan A, Makeen HA, Al Bratty M 2022. Protective effects of apigenin on methylmercury-induced behavioral/neurochemical abnormalities and neurotoxicity in rats. *Human & Experimental Toxicology*, 41: 09603271221084276. https://doi.org/10.1177/09603271221084276

Yildirim IG, Dogan F, Sanlier N 2023. Neurodegenerative diseases and phytochemicals. *Beslenme ve Diyet Dergisi*, 51: 111-118. https://doi.org/10.33076/2023. BDD. 1738.

Ziemssen T, Akgün K, Brück W 2019. Molecular biomarkers in multiple sclerosis. *Journal of Neuroinflammation*, 16(1): 272. https://doi.org/10.1186/s12974-019-1674-2

Zierfuss B, Larochelle C, Prat A 2024. Blood–brain barrier dysfunction in multiple sclerosis: Causes, consequences, and potential effects of therapies. *The Lancet Neurology*, 23(1): 95-109. https://doi.org/10.1016/S1474-4422(23)00377-

Paper received for publication in July, 2025
Paper accepted for publicaiton in January, 2026

SUPPLEMENTARY DATA

Table 1: Docking analysis of compounds

Target Proteins	*Phytochemicals*																				
	A	*B*	*C*	*D*	*E*	*F*	*G*	*H*	*I*	*J*	*K*	*L*	*M*	*N*	*O*	*P*	*Q*	*R*	*S*	*T*	*U*
CXCL10	-10.6			-9.3	10.3			-10.1						-9.8		-9.1			-9.3		
MMP-3	-10.6	-9.1	-10.4		-10.5		-9.3	-9.4	-9.3		-9.2	-9.7		-9.3		-9.1	-9	-9.1			
CD20	-9.4				-9.6																
sNfL	-10.2													-9.1							
MOG	-9.4																				
IsoP- F2α	-9.3				-9.7			-9.2						-9.7							
MMP-2	-9.7	-9.2		-9.4	-9.1			-9.6		-9.1			-9.6	-9.6		-9					
LC3-II																					
DHODH	-9.4	-9.9	-9.5	-9	-9.5	-9.4	-9.8		-9.1		-9.8	-9.5		-9				-9.1			
HSP70	-9.5							-9						-9.3							
CD50	-9.1																				
HSP32		-9.2																			
Amyloid β (Aβ)		-9.3			-9.5			-9.1													
Protein Carbonyls	-9.5	-9.1		-9.5				-9.7	-9.2			-9.2						-9.5			
PAD4								-9.3													
MMP-9	-10.4	-9.4		-9.5	-9.5		-9.6	-10	-10.3		-9.7	-10.1		-9	-9		-9.1	-9.6			

Abbreviations: A-Hesperidin, B-Epicatechin Gallate, C-Onosmin, D-Isoorientin, E-Procyanidin, F-THC, G-Naringnin, H-Catechin Gallate, I-Quercetin, J-Vitexin, K-Apiginin, L-Luteolin, M-Stigmasterol, N-Rutin, O-Kaempferol, P-Hyproside, Q-Isorhamnetin, R-Myricetin, S-Arjunolic Acid, T-CBD, U-Artemisinin

Table 2: Swiss ADME and drug-likeness analysis

Pharmacokinetics	*Epicatechin Gallate*	*Onosmin*	*THC*	*Naringin*	*Vitexin*	*Apigenin*	*Stigmasterol*	*Rutin*	*Kaempferol*	*Hyproside*	*Isorhamnetin*	*Myricetin*	*Arjunolic Acid*
MW	442.37	241.29	314.46	272.25	432.38	270.24	412.69	610.52	286.24	464.38	316.26	318.24	488.7
H-bond acceptors	10	2	2	5	10	5	1	16	6	12	7	8	5
H-bond doners	7	2	1	3	7	3	1	10	4	8	4	6	4
MR	110.04	72.16	97.91	71.57	106.61	73.99	132.75	141.38	76.01	110.16	82.5	80.06	138.98
Silicos-IT Log P	1.04	2.97	5.41	2.05	0.33	2.52	6.86	-2.11	2.03	-0.59	2.06	1.06	4.35
Atoms	32	18	23	20	31	20	30	43	21	33	23	23	35
Lipinski #violations	1	2	1	0	1	0	1	3	0	2	0	1	0
BBB	No	Yes	Yes	No	No	No	No	No	No	No	No	No	No

Table 3i: Phytochemical analysis of compound

AdmetSAR Analysis												
Properties	*Epicatechin Gallate*		*Onosmin*		*THC*		*Naringin*		*Vitexin*		*Apigenin*	
BBB (Bain-Blood Barriers)	-	0.6047	+	0.8295	+	0.9685	+	0.6794	-	0.6472	+	0.6364
Intestinal absorption	HIA+		HIA+		HIA+		HIA+		HIA+		HIA+	
Caco-2 Permeability	Caco2-		Caco2+		Caco2+		Caco2+		Caco2-		Caco2+	
P-glycoprotein	Substrate		Non-substrate		Substrate		Substrate		Substrate		Non-substrate	
P-glycoprotein Inhibitor	Non-inhibitor		Non-inhibitor		Non-inhibitor		Non-inhibitor		Non-inhibitor		Non-inhibitor	
Biodegradation	Not-ready biodegradable		Not-ready biodegradable		Not-ready biodegradable		Not-ready biodegradable		Not-ready biodegradable		Not-ready biodegradable	
Aqueous solubility (Logs)	-3.3141				-4.3219		-3.1905		-2.3978		-2.7765	
AMES Toxicity	Non-AMES toxic		Non-AMES toxic		Non-AMES toxic		Non-AMES toxic		AMES toxic		Non-AMES toxic	
ProTox-3 Prediction												
Hepatotoxicity	Inactive		Inactive		Inactive		Inactive		Inactive		Inactive	
Carcinogenicity	Inactive		Inactive		Inactive		Inactive		Inactive		Inactive	
Immunotoxicity	Inactive		Inactive		Active		Inactive		Inactive		Inactive	
Mutagenicity	Inactive		Inactive		Inactive		Inactive		Active		Inactive	
Cytotoxicity	Inactive		Inactive		Inactive		Active		Inactive		Inactive	
BBB-barrier	Active	0.53	Active	0.68	Active	0.92	Active	0.52	Inactive	0.55	Inactive	0.51

Table 3ii: Phytochemical analysis of compound

AdmetSAR Analysis										
Properties	*Stigma sterol*		*Rutin*		*Kaempferol*		*Hyperoside*		*Isorhamnetin*	
BBB (Bain-Blood Barriers)	+	0.9743	-	0.8542	-	0.543	-	0.604	-	0.571
Intestinal absorption	HIA+		HIA+		HIA+		HIA+		HIA+	
Caco-2 Permeability	Caco2+		Caco2-		Caco2-		Caco2-		Caco2-	
P-glycoprotein	Substrate		Substrate		Substrate		Substrate		Substrate	
P-glycoprotein Inhibitor	Inhibitor		Non-inhibitor		Non-inhibitor		Non-inhibitor		Non-inhibitor	
Biodegradation	Not-ready biodegradable		Not-ready biodegradable		Not-ready biodegradable		Not-ready biodegradable		Not-ready biodegradable	
Aqueous solubility (Logs)	-4.7027		-2.7724		-3.2563		-3.3141		-2.9994	
AMES Toxicity	Non-AMES toxic		AMES toxic		Non-AMES toxic		Non-AMES toxic		Non-AMES toxic	
ProTox-3 Prediction										
Hepatotoxicity	Inactive		Inactive		Inactive		Inactive		Inactive	
Carcinogenicity	Inactive		Inactive		Inactive		Inactive		Inactive	
Immunotoxicity	Active		Active		Inactive		Active		Active	
Mutagenicity	Inactive		Inactive		Inactive		Inactive		Inactive	
Cytotoxicity	Inactive		Inactive		Inactive		Inactive		Inactive	
BBB-barrier	Active	0.91	Inactive	0.75	Active	0.57	Active	0.57	Active	0.52

Table 4: Target proteins with PDB I'D

TARGETS			
Nogo-A	*5O0N*	*Integrin á4â1*	*1DPK*
Beclin-1	3DVU	VCAM-1	1IJ9
LC3-II	8T2L	CD20	3GIZ
Protein Carbonyls	4Z3D	CD52	1BEY
Vitamin-D3	2GJ5	DHODH	2PRM
AOPPs	5MND	IL6	8UPA
HSP70	4PO2	IL17AF	5N92
HSP90	1SF8	IL1â	9ILB
HSP60	1SRV	MMP-2	1EAK
HSP27	6GJH	MMP-9	2OVX
HSPB5	6BP9	MMP-3	2D1O
HSP32	1N45	Lingo-1	4OQT
SOD	1P7G	GFAP	6A9P
GSH	7SO8	MBP	2MH8
CAT	1PD5	MOG	2F7Y
MDA	5IRB	PLP 1	4ATP
IsoP- F2á	5JRL	NADPH Oxidase	7CFZ
8-OHdG	3F10	LCN2	3BX8
4-HNE	2K8U 3t6h	CXCL10	8K2X
TNF-á	1a8m	PAD2	4N22
TGF*â*1	1KSQ	PAD4	3APM
sNfL	2M9Y 8SHC	Amyloid â (Aâ)	6GHX

Table 5: Screened phytocompounds with C-ID

Phytocompounds and C-ID			
Onosmin	11425005	Isoorientin	114776
Artemisinin	68827	Isorhamnetin	5281654
Arjunolic acid	73641	Vitexin	5280441
CBD	644019	Naringenin	439246
THC	16078	Catechin Gallate	5276454
Stigmasterol	5280794	Epicatechin Gallate	107905
Apigenin	5280443	Rutin	5280805
Hesperidin	10621	Quercetin	5280343
Myricetin	5281672	Ferulic Acid	445858
Hyperoside	5281643	Luteolin	5280445
Procyanidin B2	122738	Kaempferol	5280863

Table 6: Levels of TNF-á, IL-6, IL-17AF, IL-1â, IL-17 and HSP27 in MS-induced rats treated with Exosomal Phytochemicals (EPCs)

Groups	*TNF-á (pg/mL)*	*IL-6 (pg/mL)*	*IL-17AF (pg/mL)*	*IL-1â (pg/mL)*	*IL-17 (pg/mL)*	*HSP27 (pg/mL)*
Control	21.25±5.66 a	10.59±2.15 a	5.29±1.09 a	8.99±1.78 a	4.88±0.95 a	12.35±2.98 a
+Control (Exosome Vehicle)	45.88±8.49 d	35.21±6.29 d	22.49±3.95 d	31.55±4.89 d	20.33±3.72 d	39.12±6.41 d
Onosmin-Exosome	31.29±4.78 c	22.55±4.39 c	13.78±2.85 c	20.92±3.42 c	12.99±2.51 c	27.35±4.95 c
THC-Exosome	27.59±5.19 b	18.89±3.78 bc	11.33±2.42 bc	16.59±2.98 bc	10.99±2.31 bc	22.45±3.99 bc
Naringnin-Exosome	24.59±4.49 b	15.79±3.55 b	9.99±2.21 b	14.88±2.55 b	9.55±1.89 b	20.15±3.79 b
Apiginin-Exosome	28.59±7.35 bc	20.32±4.85 bc	12.45±2.69 bc	18.99±3.42 bc	11.85±2.41 bc	24.59±4.39 bc
Stigmasterol-Exosome	29.55±4.59 a	21.12±4.22 bc	13.12±2.55 bc	19.42±3.69 bc	12.45±2.18 bc	26.35±4.58 bc
Diroximel	35.19±8.59 bc	25.88±5.21 c	15.79±3.12 c	23.45±4.29 c	14.65±2.79 c	30.75±5.55 c
p-value (d"0.05)	0.021	0.032	0.028	0.030	0.025	0.027
LSD (d"0.05)	6.89	5.75	3.42	4.99	3.21	5.35

Table 7: Levels of MMP9, MMP2, MMP3, HSP60, HSP90 and HSP70 in MS-induced rats treated with Exosomal Phytochemicals (EPCs)

Groups	*MMP-9 (ng/mL)*	*MMP-2 (ng/mL)*	*MMP-3 (ng/mL)*	*HSP60 (ng/mL)*	*HSP90 (ng/mL)*	*HSP70 (ng/mL)*
Control	12.35±2.98 a	8.25±1.89 a	5.75±1.45 a	10.89±2.11 a	14.99±2.78 a	9.55±1.89 a
+Control (Exosome Vehicle)	35.42±5.78 d	27.88±4.99 d	19.65±3.55 d	30.25±5.19 d	38.42±6.33 d	25.89±4.42 d
Onosmin-Exosome	22.59±3.89 c	18.75±3.49 c	12.33±2.88 c	21.42±3.95 c	26.55±4.89 c	17.95±3.42 c
THC-Exosome	18.99±3.25 bc	15.89±2.99 bc	10.25±2.55 bc	17.35±3.42 bc	21.99±3.78 bc	14.78±2.89 bc
Naringnin-Exosome	16.75±2.98 b	13.42±2.65 b	8.99±2.11 b	14.92±2.99 b	18.75±3.42 b	12.35±2.55 b
Apigenin-Exosome	17.32±2.99 b	14.01±2.78 b	9.23±2.34 b	15.45±2.78 b	19.23±3.29 b	13.12±2.68 b
Stigmasterol-Exosome	19.45±3.42 bc	16.25±3.12 bc	10.98±2.77 bc	16.89±3.23 bc	22.45±3.65 bc	15.23±3.02 bc
Diroximel	21.12±3.77 c	17.89±3.55 c	11.78±2.89 c	19.23±3.65 c	24.12±4.12 c	16.78±3.19 c
p-value (d"0.05)	0.027	0.034	0.029	0.031	0.026	0.028
LSD (d"0.05)	4.55	3.89	2.75	3.99	4.45	3.25

Table 8: Levels of Integrin á4â1, VCAM-1, TGFâ1, NADPH Oxidase, Vitamin-D3, and HSP32 in MS-induced rats treated with Exosomal Phytochemicals (EPCs)

Groups	*Integrin á4â1 (ng/mL)*	*VCAM-1 (ng/mL)*	*TGFâ1 (pg/mL)*	*NADPH Oxidase (µmol/min/mg)*	*Vitamin-D3 (ng/mL)*	*HSP32 (ng/mL)*
Control	8.25±1.45 a	12.55±2.98 a	15.42±3.12 a	5.75±1.22 a	28.35±4.11 a	10.99±2.32 a
+Control (Exosome Vehicle)	22.88±3.99 d	34.42±5.78 d	40.25±5.99 d	19.65±3.55 d	12.42±3.35 d	30.55±5.19 d
Onosmin-Exosome	15.75±2.99 c	25.88±4.49 c	30.99±4.35 c	12.33±2.88 c	18.75±3.42 c	22.78±3.89 c
THC-Exosome	12.99±2.55 bc	21.42±3.99 bc	25.75±4.11 bc	10.25±2.55 bc	22.99±3.78 bc	19.35±3.42 bc
Naringnin-Exosome	11.55±2.35 b	18.75±3.55 b	22.99±3.78 b	8.99±2.11 b	24.75±3.99 b	16.89±3.25 b
Apiginin-Exosome	14.42±3.11 bc	23.35±4.22 bc	28.55±4.78 bc	11.42±2.89 bc	20.42±3.55 bc	21.22±3.89 bc
Stigmasterol-Exosome	13.75±2.78 bc	20.99±3.78 bc	27.42±4.55 bc	10.99±2.78 bc	21.99±3.72 bc	18.75±3.66 bc
Diroximel	17.89±3.49 c	28.42±4.88 c	32.55±5.19 c	14.99±3.11 c	16.55±3.42 c	24.99±4.42 c
p-value (d”0.05)	0.018	0.025	0.021	0.019	0.022	0.024
LSD (d”0.05)	3.75	4.99	5.25	2.95	3.55	4.22

Table 9: Levels of MBP, DHODH, PAD4, LCN2 and Beclin-1 in MS-induced rats treated with Exosomal Phytochemicals (EPCs)

Groups	*MBP (ng/mL)*	*DHODH (U/L)*	*PAD4 (pg/mL)*	*LCN2 (ng/mL)*	*Beclin-1 (pg/mL)*
Control	42.59±3.12 a	5.62±0.87 a	3.28±0.45 a	2.45±0.36 a	4.12±0.51 a
+Control (Exosome Vehicle)	19.24±2.98 d	12.76±1.09 d	7.89±0.74 d	8.15±1.03 d	9.45±1.12 d
Onosmin-Exosome	36.14±3.51 b	7.89±1.02 bc	4.12±0.63 b	3.89±0.54 b	5.98±0.67 b
THC-Exosome	38.79±4.02 bc	6.98±0.92 b	4.52±0.78 bc	4.12±0.68 b	6.23±0.74 bc
Naringnin-Exosome	40.24±3.76 bc	6.12±0.88 ab	3.98±0.57 bc	3.62±0.49 b	5.47±0.63 bc
Apiginin-Exosome	37.45±4.09 b	7.36±0.99 bc	4.65±0.72 bc	4.34±0.58 bc	6.12±0.71 bc
Stigmasterol-Exosome	35.98±3.83 b	8.12±1.03 c	4.98±0.69 c	4.76±0.64 bc	6.78±0.85 c
Diroximel	31.57±4.21 c	9.24±1.08 c	5.23±0.81 c	5.12±0.78 c	7.25±0.92 c
p-value (d”0.05)	0.018	0.025	0.031	0.022	0.027
LSD (d”0.05)	3.42	1.35	0.91	0.87	1.02

Table 10: Expression levels of PLP1, PAD2, Lingo-1, Nogo-A and GFAP in MS-induced rats treated with Exosomal Phytochemicals (EPCs)

Groups	*PLP1 (ng/mL)*	*PAD2 (pg/mL)*	*Lingo-1 (pg/mL)*	*Nogo-A (pg/mL)*	*GFAP (ng/mL)*
Control	45.12±3.27 a	3.98±0.56 a	2.36±0.41 a	1.98±0.32 a	5.12±0.67 a
+Control (Exosome Vehicle)	20.78±2.89 d	9.12±1.04 d	8.24±0.89 d	7.98±1.02 d	11.36±1.21 d
Onosmin-Exosome	38.56±3.89 b	5.76±0.83 b	3.78±0.54 b	3.12±0.49 b	6.78±0.88 b
THC-Exosome	40.23±4.02 bc	5.12±0.79 b	3.45±0.61 b	2.98±0.52 b	6.23±0.74 bc
Naringnin-Exosome	42.11±3.98 bc	4.87±0.72 ab	3.12±0.49 ab	2.78±0.47 ab	6.12±0.71 bc
Apiginin-Exosome	39.65±4.17 b	5.89±0.85 bc	3.89±0.58 bc	3.34±0.59 b	7.02±0.83 bc
Stigmasterol-Exosome	37.78±3.91 b	6.24±0.91 bc	4.02±0.63 bc	3.56±0.61 bc	7.78±0.96 c
Diroximel	32.67±4.23 c	7.14±0.98 c	4.65±0.75 c	4.12±0.68 c	8.12±1.02 c
p-value (dˆ0.05)	0.019	0.026	0.033	0.021	0.028
LSD (dˆ0.05)	3.48	1.28	0.94	0.87	1.05

Table 11: Levels of Protein Carbonyls, NF-êB, MDA, 8-OHdG, and IsoP-F2á in MS-induced rats treated with Exosomal Phytochemicals (EPCs)

Groups	*Protein Carbonyls (nmol/mg)*	*NF-êB (pg/mL)*	*MDA (nmol/mL)*	*8-OHdG (ng/mL)*	*IsoP-F2á (pg/mL)*
Control	1.25±0.45 a	15.55±3.22 a	2.42±0.88 a	3.75±1.22 a	9.99±2.11 a
+Control (Exosome Vehicle)	4.88±1.02 d	38.42±5.78 d	7.99±2.35 d	10.25±2.88 d	29.55±4.89 d
Onosmin-Exosome	3.15±0.89 c	27.99±4.42 c	5.75±1.45 c	7.22±1.99 c	21.78±3.55 c
THC-Exosome	2.75±0.72 bc	24.42±3.99 bc	4.99±1.32 bc	6.15±1.75 bc	18.35±3.22 bc
Naringnin-Exosome	2.42±0.65 b	21.75±3.42 b	4.25±1.11 b	5.42±1.55 b	15.75±3.11 b
Apiginin-Exosome	2.99±0.78 bc	26.35±4.11 bc	5.22±1.22 bc	6.78±1.88 bc	19.42±3.45 bc
Stigmasterol-Exosome	2.85±0.69 bc	23.99±3.78 bc	5.05±1.18 bc	6.42±1.78 bc	17.75±3.35 bc
Diroximel	3.55±0.88 c	30.42±4.55 c	6.15±1.75 c	8.22±2.11 c	24.99±3.89 c
p-value (dŠ0.05)	0.019	0.022	0.020	0.021	0.023
LSD (dŠ0.05)	0.85	4.22	1.12	1.88	3.55

Table 12: Levels of Amyloid â, GSH, LC3-II, HSPB5 and CXCL10 in MS-induced rats treated with Exosomal Phytochemicals (EPCs)

Groups	*Amyloid â (Aâ) (ng/mL)*	*GSH (µmol/g)*	*LC3-II (pg/mL)*	*HSPB5 (pg/mL)*	*CXCL10 (pg/mL)*
Control	1.12±0.21 a	8.98±1.24 a	3.45±0.56 a	6.89±1.02 a	12.34±2.01 a
+Control (Exosome Vehicle)	3.89±0.56 d	3.14±0.78 d	9.78±1.03 d	3.12±0.67 d	28.56±3.12 d
Onosmin-Exosome	2.45±0.38 c	6.78±0.98 b	5.67±0.89 bc	5.23±0.89 bc	18.34±2.78 bc
THC-Exosome	2.23±0.34 bc	7.12±1.02 bc	4.98±0.76 b	5.67±0.91 b	16.45±2.56 bc
Naringnin-Exosome	2.12±0.29 bc	7.56±1.08 bc	4.87±0.71 b	6.12±0.94 bc	15.78±2.34 b
Apiginin-Exosome	2.67±0.42 bc	6.89±0.99 bc	5.12±0.82 bc	5.34±0.87 bc	17.23±2.61 bc
Stigmasterol-Exosome	2.78±0.47 bc	6.45±0.94 bc	5.34±0.86 bc	5.12±0.85 bc	19.12±2.98 c
Diroximel	3.12±0.53 c	5.89±0.88 c	6.12±0.94 c	4.78±0.79 c	21.34±3.12 c
p-value (d—0.05)	0.018	0.025	0.030	0.022	0.027
LSD (d—0.05)	0.56	1.12	1.04	0.98	2.34

Table 13: Levels of SOD, CAT, MOG, 4-HNE, and sNfL in MS-induced rats treated with Exosomal Phytochemicals (EPCs)

Groups	*SOD (U/mg)*	*CAT (U/mg)*	*MOG (ng/mL)*	*4-HNE (nmol/mL)*	*sNfL (pg/mL)*
Control	18.55±3.22 a	25.75±4.55 a	5.42±1.22 a	2.99±0.88 a	8.25±2.55 a
+Control (Exosome Vehicle)	7.88±2.45 d	10.55±3.12 d	15.22±2.88 d	8.75±2.42 d	25.35±4.88 d
Onosmin-Exosome	12.42±3.11 c	18.75±4.22 c	10.42±2.45 c	5.75±1.75 c	18.78±3.99 c
THC-Exosome	14.22±3.45 bc	21.42±4.55 bc	8.99±2.11 bc	4.99±1.55 bc	15.88±3.42 bc
Naringnin-Exosome	16.35±3.78 b	23.75±4.78 b	7.55±1.99 b	4.25±1.32 b	13.42±3.22 b
Apiginin-Exosome	13.99±3.65 bc	20.88±4.35 bc	9.42±2.22 bc	5.22±1.45 bc	17.42±3.65 bc
Stigmasterol-Exosome	14.88±3.55 bc	22.25±4.49 bc	8.75±2.05 bc	5.05±1.28 bc	16.42±3.55 bc
Diroximel	11.75±3.12 c	17.99±4.15 c	11.22±2.65 c	6.15±1.75 c	20.25±4.22 c
p-value (d”0.05)	0.018	0.020	0.021	0.022	0.023
LSD (d”0.05)	2.45	4.12	2.22	1.45	3.88

Table 14: Pearson Correlation matrix of significant and strong associations [highly correlated variable pairs (|r| > 0.95)] among variables in MS-induced rats treated with exosomal phytochemicals (EPCs)

Variable 1	*Variable 2*	*Correlation (r)*
TNF-á	IL-6	0.962**
TNF-á	IL-17AF	0.944*
TNF-á	IL-1â	0.933*
TNF-á	HSP27	0.947*
TNF-á	MMP-9	0.951**
TNF-á	MMP-2	0.936*
TNF-á	HSP90	0.940*
IL-6	IL-17AF	0.958**
IL-6	HSP27	0.960**
IL-6	MMP-9	0.965**
IL-6	MMP-2	0.949*
IL-6	HSP90	0.953**
IL-17AF	IL-1â	0.947*
Integrin á4â1	VCAM-1	0.958**
Integrin á4â1	Protein Carbonyls	0.949*
Integrin á4â1	NF-êB	0.972***
Integrin á4â1	MDA	0.967**
Integrin á4â1	IsoP-F2á	0.966**
Integrin á4â1	SOD	–0.948*
Integrin á4â1	Vitamin D3	–0.945*
VCAM-1	Protein Carbonyls	0.955**
VCAM-1	NF-êB	0.987***
VCAM-1	MDA	0.957**
VCAM-1	IsoP-F2á	0.962**
VCAM-1	SOD	–0.930*
NF-êB	MDA	0.974***
NF-êB	IsoP-F2á	0.970***
NF-êB	SOD	–0.958**
NF-êB	Vitamin D3	–0.959**
Protein Carbonyls	IsoP-F2á	0.950**
Protein Carbonyls	SOD	–0.947*
MDA	IsoP-F2á	0.964**
MDA	SOD	–0.943*
IL-1â	MMP-9	0.951**
MBP	PLP1	0.945*

Significance level: $p < 0.01$ (highly significant) denoted as **, $p < 0.05$ (significant) denoted as *

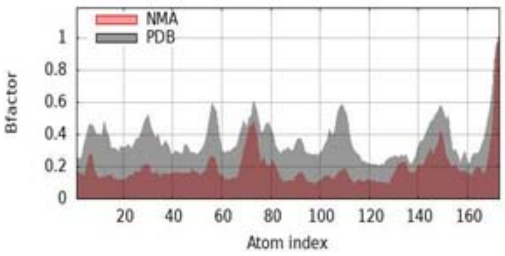

(A) **(B)**

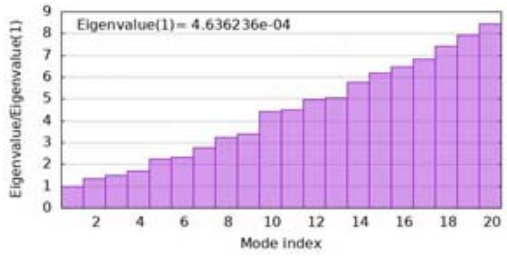

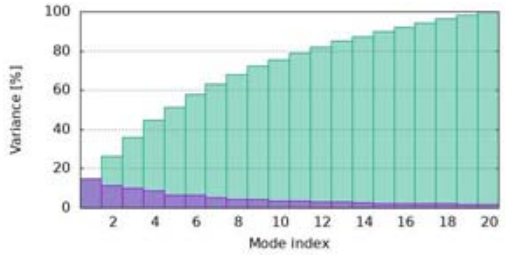

(C) **(D)**

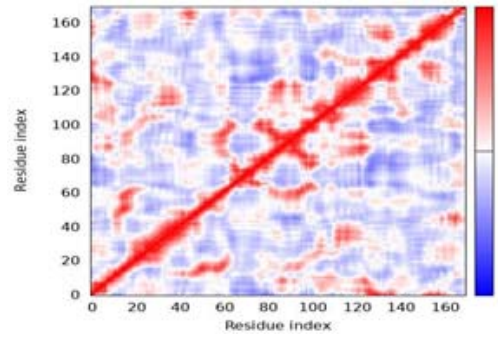

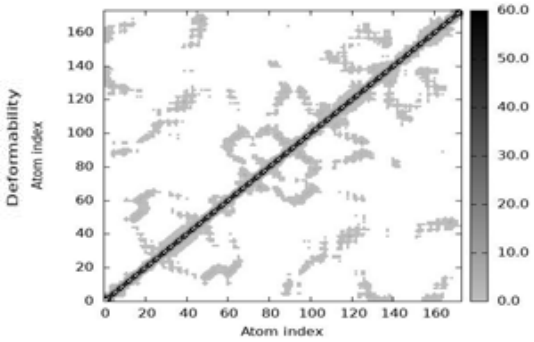

(E) **(F)**

1 (i) **(F)**

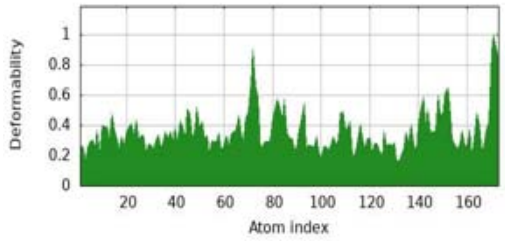

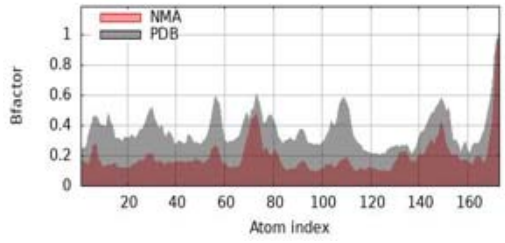

(A) **(B)**

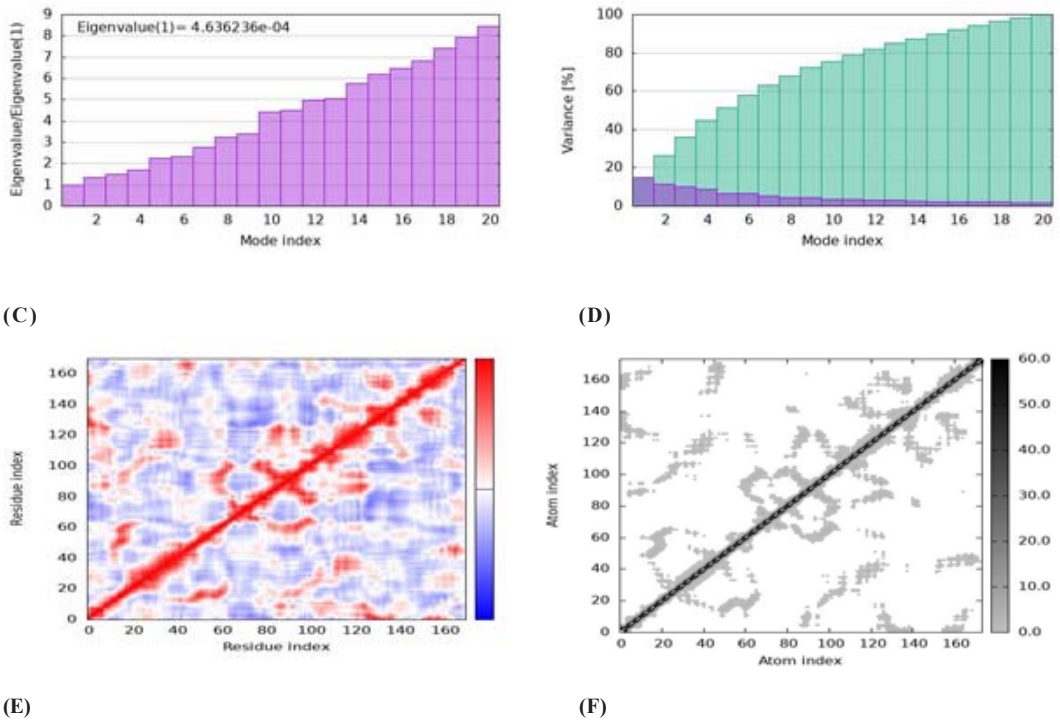

Fig. 1. (I-II) Dynamic analysis of the protein (MMP-3) ligand Complex (Naringnin and Apiginin)

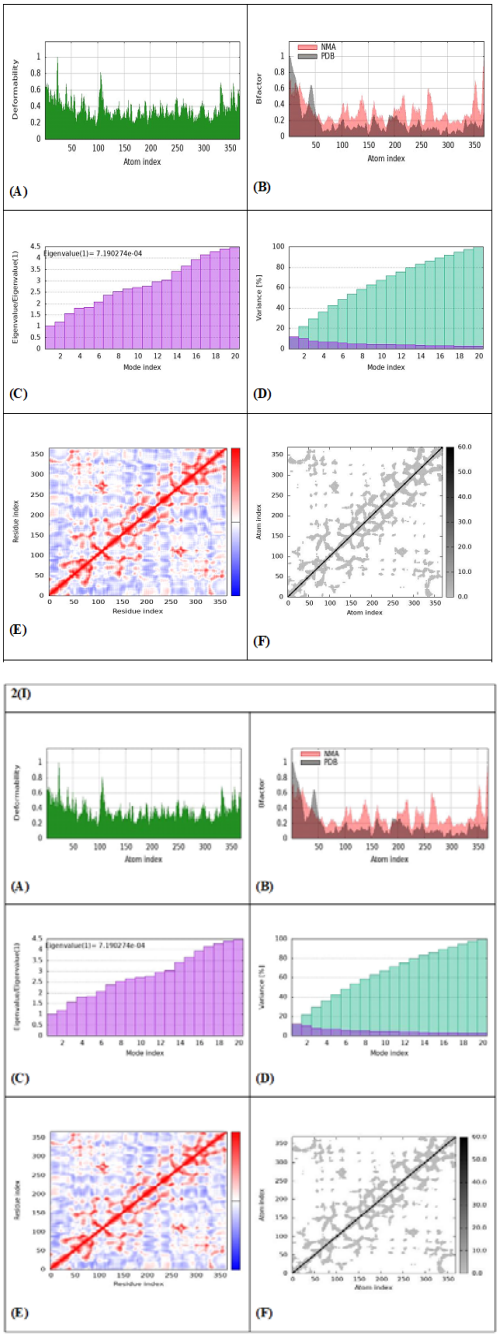

Fig. 2. (I-II) Dynamic analysis of the protein (DHODH) ligand Complex (Onosmin and THC)

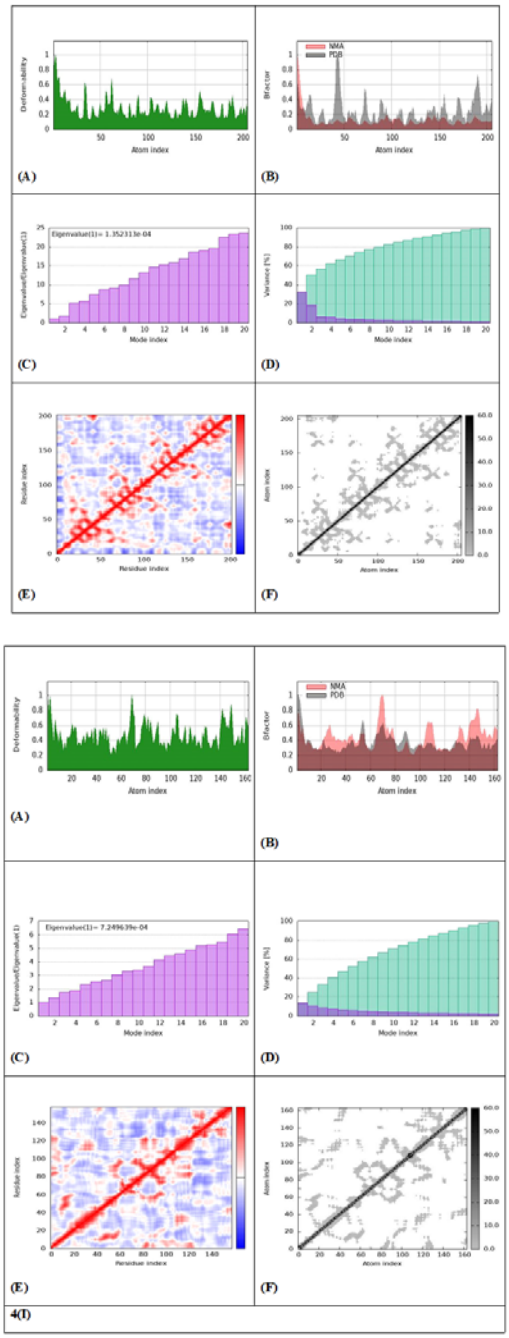

Fig. 3. Dynamic analysis of the protein (MMP-2) ligand Complex (Stigmasterol)

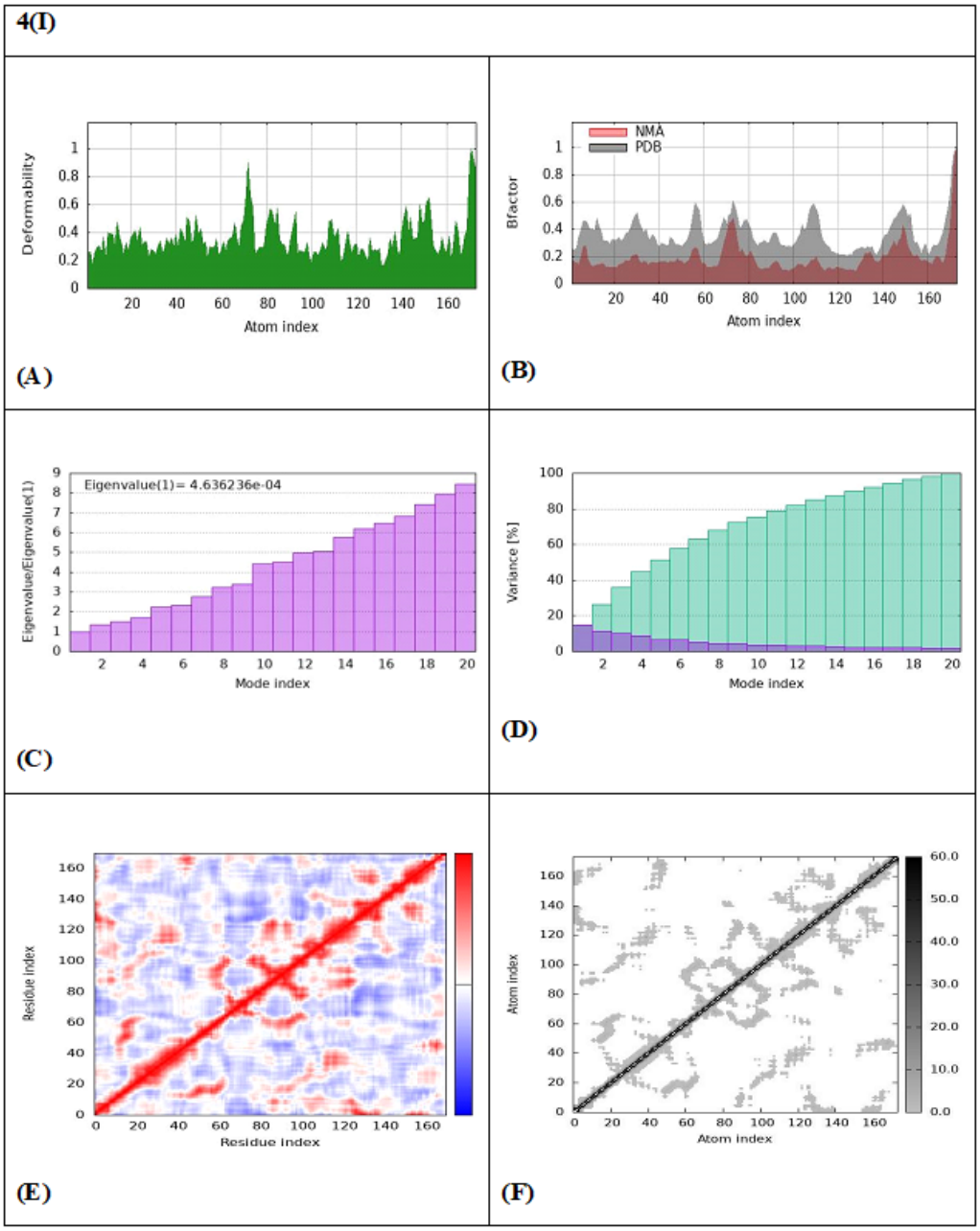

Fig. 4. (I-II): Dynamic analysis of the protein (MMP-9) ligand Complex (Naringnin and Apiginin)